RADC-TR-65-147
Final Report

A SURVEY OF TRANSIENT RADIATION-EFFECT STUDIES ON MICROELECTRONICS

W. C. Bowman
R. S. Caldwell
G. W. Svetich

TECHNICAL REPORT NO. RADC-TR-65-147
May 1965

Development Engineering Branch
Rome Air Development Center
Research and Technology Division
Air Force Systems Command
Griffiss Air Force Base, New York

When US Government drawings, specifications, or other data are used for any purpose other than a definitely related government procurement operation, the government thereby incurs no responsibility nor any obligation whatsoever; and the fact that the government may have formulated, furnished, or in any way supplied the said drawings, specifications, or other data is not to be regarded by implication or otherwise, as in any manner licensing the holder or any other person or corporation, or conveying any rights or permission to manufacture, use, or sell any patented invention that may in any way be related thereto

DDC release to CFSTI is not authorized.

All distribution of this report is controlled. Qualified Defense Documentation Center users will request through RADC (EMEAS), Griffiss AFB, NY.
The distribution of this report is limited because it contains test backup data which would assist an enemy in the reduction of our lead time.

Foreign announcement and distribution of this report is not authorized.

This research was sponsored by the
DEFENSE ATOMIC SUPPORT AGENCY
under NWER Subtask 16.027.

Do not return this copy. Retain or destroy.

A SURVEY OF TRANSIENT RADIATION-EFFECT STUDIES ON MICROELECTRONICS

W. C. Bowman
R. S. Caldwell
G. W. Svetich

AIR FORCE, Cato Show Prtg. Co. 5/26/66 - 315 -

FOREWORD

This report was prepared by The Boeing Company, Seattle, Washington, on Air Force Contract AF 30(602)-3585 under DASA Subtask No. 16.027 of Project No. 5710. The work was administered under the direction of the Rome Air Development Center, Engineering Division. Technical monitoring of the contract was performed by Mr. Arthur W. Desens (EMEAS). The report preparation portion of the contract was monitored by Mr. Paul B. Richards (EMEAS).

This study was begun in January 1965 and concluded in April 1965; the report was submitted on April 29, 1965. The work was performed by personnel of the Radiation Effects Unit, Nuclear and Space Physics organization of The Boeing Company's Aero-Space Division.

Contributors to the report were:

Dr. W. C. Bowman	Principal author
Dr. R. S. Caldwell	Technical Leader, author
Dr. G. W. Svetich	Abstracting
Mr. K. E. Kells	Initial contacts
Mr. R. T. Aquino	Initial contacts

This report completes the work on Item 1 under Contract AF 30(602)-3585.

This technical report has been reviewed and is approved:

Approved: Daniel R. Loreto
DANIEL R. LORETO
Chief, Development Engineering Branch
Engineering Division

Approved: Joseph Marecky
WILLIAM P. BETHKE
Chief, Engineering Division

FOR THE COMMANDER: Irving J. Gabelman
IRVING J. GABELMAN
Chief, Advanced Studies Group

ABSTRACT

In order to obtain complete up-to-date knowledge of the work accomplished and presently being done on the effects of transient nuclear radiation on microelectronics, a survey of the laboratories investigating this subject was conducted. Telephone contacts were made with specific individuals in 53 different laboratories. Data were obtained by means of questionnaires, reports, and personal visits. Abstracts of each document or other data source are included in the report. The abstracts describe the devices tested and the test environment, the type of dosimetry used, the general results obtained, and provide other relevant information. Summaries of failure levels are given in the abstracts whenever the information was readily available. A tabulated summary of the devices tested and the test conditions is presented. Failure levels observed by different investigators are compared for a few duplicated devices. Nine classified abstracts are contained in a supplement to the main report.

TABLE OF CONTENTS

		Page
SECTION I	INTRODUCTION	1
SECTION II	PERSPECTIVE	8
SECTION III	SUMMARY	11
SECTION IV	ABSTRACTS	41
	Abstract 1: American Bosch-Arma	42
	Abstract 2: Autonetics	43
	Abstract 3: Autonetics	46
	Abstract 4: Battelle Memorial Institute	47
	Abstract 5: Bell Telephone Laboratories, Inc.	48
	Abstract 6: The Bendix Corporation	50
	Abstract 7: The Boeing Company	52
	Abstract 8: The Boeing Company	55
	Abstract 9: The Boeing Company	67
	Abstract 10: The Boeing Company	69
	Abstract 11: Burroughs Corporation	70
	Abstract 12: Burroughs Corporation	72
	Abstract 13: Douglas Aircraft Company	74
	Abstract 14: Douglas Aircraft Company	77
	Abstract 15: General Atomic	79
	Abstract 16: General Atomic	80
	Abstract 17: General Atomic	82
	Abstract 18: General Atomic	88
	Abstract 19: General Atomic	90
	Abstract 20: Honeywell, Inc.	91
	Abstract 21: Honeywell, Inc.	93
	Abstract 22: Honeywell, Inc.	94
	Abstract 23: Hughes Aircraft Company	95
	Abstract 24: Johns Hopkins University Applied Physics Laboratory	98
	Abstract 25: Ling-Temco-Vought	100
	Abstract 26: Litton Systems, Inc.	101
	Abstract 27: Lockheed-Georgia Co.	103
	Abstract 28: Lockheed Missiles and Space Company	104
	Abstract 29: Motorola	105
	Abstract 30: NASA-Langley Research Center	106
	Abstract 31: Northrop-Ventura	107
	Abstract 32: Texas Instruments, Inc.	109
	Abstract 33: U. S. Army Electronics Laboratories	110
	Abstract 34: U. S. Naval Radiological Defense Laboratory	111

LIST OF ILLUSTRATIONS

No.	Title	Page
1	Transistor gain degradation under neutron irradiation for Sylvania SNG3 gate	42
2	Test circuit	44
3	Generalized equivalent circuit of a diffused resistor	44
4	Simplified equivalent circuit (substrate grounded)	44
5	Photocurrent versus bias voltage for Fairchild resistors μER-1	45
6	Peak photocurrent versus bias voltage for thin-film and CPC resistors	45
7	Radiation response of I_{CBO} and h_{fe} of integrated transistors of types 1 and 2	49
8	General Microelectronics Type D412 NOR gate	51
9	Observed secondary photocurrent in SN511 transistor during 480-kv pulse at 10^7 rad/sec for 0.2 μsec	54
10	Observed voltage dependences of capacitance and primary photocurrents in SN511 capacitor during 480-kv X-ray pulse at 10^7 rad/sec for 0.2 μsec	54
11	SN510	56
12	Neutron degradation of voltage levels at the output for μL903	63
13	Neutron degradation of rise and fall times for μL903	64
14	Topological equivalent circuit for MHM3001	65
15	Measured and predicted response for MHM3001 with output logic level "1"	66
16	ECL and RTL output voltage versus neutron exposure	71
17	Test circuit of dual two-input RTL gate	72
18	Circuit interconnection scheme	75
19	Output voltage change versus integrated neutron flux (SCIC three-input NAND gate)	76
20	Bit loss versus integrated neutron flux (SCIC binary counter)	76

LIST OF TABLES

No.	Title	Page
I	Companies and Laboratories Contacted for Survey Data	2
II	Index of Circuits Tested With Pulsed Ionizing Radiation	12
III	Index of Circuits Tested With Neutron Radiation	29
IV	Index of Circuits Tested With Steady-State Ionizing Radiation	38
V	Comparison of Data Obtained by Different Workers	40
VI	Collector-to-Base Breakdown Voltage for X-ray Irradiated Devices	50

LIST OF TABLES (Continued)

No.	Title	Page
VII	Microcircuit Survey	57
VIII	Neutron-Irradiated Microcircuits	62
IX	Proposed SABRE System Components Tested	68
X	Transient Experiment Data	73
XI	Summary of Neutron Damage	78
XII	Summary of Power Supply Currents in Various Circuits	80
XIII	Summary of Circuit Switching Levels	81
XIV	Summary of Permanent Damage Data	81
XV	Integrated Circuits Tested	83
XVI	Radiation Thresholds and Power Supply Currents	84
XVII	Radiation-Induced Power Supply Currents	89
XVIII	Results of Integrated Circuit Transistors Tested	97
XIX	Summary of the Usability of LINC Circuits	102
XX	Milliwatt Logic Circuits Tested	102
XXI	Flash X-ray Circuit Response	107

ABBREVIATIONS AND SYMBOLS

The abbreviations and symbols used in this report are defined as follows:

BV_{CBO}	Collector-base breakdown voltage, emitter open
BV_{CES}	Sustaining breakdown voltage, collector-emitter
C	Collector-base capacitance
DCTL	Direct-coupled transistor logic
DTL	Diode-transistor logic
E	Energy
ECL	Emitter-coupled logic
EF	Emitter follower
E_n	Neutron energy
FET	Field-effect transistor
I_B (I_b)	Base current
I_C (I_c)	Collector current
I_{CBO}	Collector-base leakage current, emitter open
I_{CEO}	Collector-emitter leakage current, base open
I_{cs}	Collector-substrate leakage current
I_D	Drain current
I_{GSS}	Gate-source leakage current, drain shorted
I_R	Diode leakage current
I_t	Output current
Meg	Megohm
Mev	Million electron volts
MOS	Metal oxide semiconductor
Q	Capacitor quality factor equal to reactance divided by leakage resistance
R	Roentgen
R_{CE}	External collector-emitter resistance
RTL	Resistor-transistor logic
SCR	Silicon-controlled rectifier

ABBREVIATIONS AND SYMBOLS (Continued)

SEM	Secondary-emission monitor
SPRF	Sandia Pulsed Reactor Facility
TRIGA	General Atomic pulsed thermal reactor
TTL	Transistor-transistor logic
UCLA	University of California, Los Angeles
V_{BE}	Base-emitter voltage
V_C	Voltage applied to capacitor
V_{CB}	Base-collector voltage
V_F	Diode voltage drop at some specified forward current
V_{off}	Input voltage for maximum output voltage
V_{on}	Input voltage for minimum output voltage
V_{SAT}	Collector-emitter voltage of saturated transistor
V_t	Emitter voltage necessary to produce output current, I_t, of 100 microamperes
Z_{in}	Input impedance
brem.	Bremsstrahlung
e^-	Electron source
e^-/cm^2	Electron fluence
ev	Electron volt
dI_{cc}	Peak transient power-supply-current
h_{FE}	Common emitter direct-current gain
h_{fe}	Common emitter small signal alternating-current gain
$\hat{I}_p$	Peak primary photocurrent
I_{pp}	Primary photocurrent
I_{sp}	Secondary photocurrent
kev	Thousand electron volts
p	Protons
p/cm^2	Proton fluence
nsec	Nanosecond

ABBREVIATIONS AND SYMBOLS (Continued)

n/cm^2	Neutron fluence
nvt	Neutron fluence
rad(C)	Energy deposited in carbon
t_f	Fall time
t_r	Rise time
β	Common emitter direct-current gain (h_{FE})
β_{AC}	Common emitter small signal alternating-current gain (h_{fe})
β_{DC}	Common emitter direct-current gain (h_{FE})
β_{dc}	Common emitter direct-current gain (h_{FE})
γ	Gamma-ray source
Φ	Total dose in roentgens
ϕ	Built-in contact potential
ΔI	Change in current

SECTION I

INTRODUCTION

In order to best determine the course of future funding for radiation effects research on microelectronics, it was first desirable to define the present state of knowledge on the subject. An attempt was made, therefore, to survey the various companies and laboratories known to be interested in or investigating radiation effects.

An initial list was compiled of persons who had attended government and IEEE conferences on radiation effects within the past 2 years. These people were contacted by telephone to determine if they had done any radiation-effect work on microcircuits or microcircuit components. If they had done such work, the classification of the work was determined and an attempt was made to obtain any existing reports. References to other work were requested in order that the list of contacts could be expanded to make it as complete as possible. When information from a laboratory was determined to exist, one of three courses of action was taken to obtain the information: (1) where reports existed and little or no activity was currently taking place, an attempt was made to obtain the reports; (2) where a large volume of work had been done or was currently being done, a plant visit was made by W. C. Bowman and/or R. S. Caldwell of The Boeing Company, accompanied by Paul Richards of the Rome Air Development Center; and (3) when reports did not exist and a plant visit was not practical, a questionnaire was sent to obtain sufficient information for the survey.

Two factors detract from the completeness of this report: First, it was impossible to gain access to a company's proprietary information. Second, some reports were not received in time to be included in the survey. In addition, there is always the possibility that some work has been overlooked. Considering these factors, it is estimated that the survey covers approximately 95 percent of the radiation-effect work accomplished at the time of this writing. Table I lists the companies and laboratories contacted, indicates the method of data collection used, and cites pertinent comments on current and future work.

Table I. Companies and Laboratories Contacted for Survey Data

Company	Contact	*				Comments
		N	Q	R	V	
1. Aberdeen Proving Grounds U. S. Army Ballistic Research Laboratory Aberdeen, Maryland	K. A. Pullin	X				
2. Aerojet General-Nucleonics San Ramon, California	Donald Toomb	X				
3. Aeroneutronics Division of Philco Newport Beach, California	Gerald Gordon, Jr.	X				
4. American Bosch-Arma Garden City, N. Y.	Bernard Gaines			X		Not currently active in radiation effects on microcircuits
5. Atomics International Canoga Park, California	A. J. Saur	X				Proposed in-house program pending
6. Autonetics Division of NAA, Inc. Anaheim, California	E. E. Griffin, Jr.				X	Unreported testing at SPRF and super flash X-ray (BSD), in-house program in progress
7. AVCO Cincinnati, Ohio	Calvin Bott	X				Presently testing two 10-Mc linear amplifiers at G. A. TRIGA
8. Battelle Institute Columbus, Ohio	D. J. Hamman	X				Presently testing 200 circuits (16 types of gates and flip-flops) for permanent damage using 3-Mev electrons (NASA)

* N = No Work Q = Questionnaire Sent R = Report Received V = Visited

Table I. Companies and Laboratories Contacted for Survey Data (Continued)

Company	Contact	*				Comments
		N	Q	R	V	
9. Bell Laboratories Whippany, N. J.	R. R. Blair			X		Unreported work at White Sands in conjunction with Ft. Monmouth (Signal Corps)
10. Bendix Corporation Research Laboratories Division Southfield, Michigan	Frank Larin		X			Not currently active in radiation effects on microcircuits
11. The Boeing Company Seattle, Washington	R. S. Caldwell H. W. Wicklein				X	Presently working on programs for RADC, BSD, and AFWL
12. Burroughs Corporation Paoli, Pennsylvania	F. T. Lynch				X	Not currently active in radiation effects on microcircuits
13. CBS Laboratories Stamford, Connecticut	Daniel Bender	X				
14. Douglas Aircraft Company Santa Monica, California	Jan Tobolski				X	Not currently active in radiation effects on microcircuits
15. EG&G Goleta, California	Wayland George	X				
16. Electro-Mechanical Research College Park, Maryland	James Holeman	X				
17. Fairchild Semiconductor Palo Alto, California	Peter Lauritzen		X			Small amount of work done (unreported; no reply)
18. General Atomic La Jolla, California	V. A. Van Lint R. A. Poll				X	

* N = No Work Q = Questionnaire Sent R = Report Received V = Visited

Table I. Companies and Laboratories Contacted for Survey Data (Continued)

Company	Contact	*				Comments
		N	Q	R	V	
19. General Dynamics Fort Worth, Texas	E. T. Smith	X				
20. General Electric Oklahoma City, Oklahoma	John Bilinski	X				Engaged in designing hardened circuits
21. Harry Diamond Laboratory Washington, D. C.	P. H. Haas	X				
22. Honeywell St. Petersburgh, Florida	Donald Siegeland			X		
23. Hughes Fullerton, California	James Bell Robert Marshall				X	Presently doing thin-film program for BUWEPS
24. IBM Owego, N. Y.	William Bohan			X		
25. Johns Hopkins Applied Physics Laboratory Silver Springs, Maryland	Arthur Hogrefe			X		Work in conjunction with The Martin Company
26. Kearfott Division General Precision, Inc. Little Falls, N. J.	Sidney Black	X				In-house program (proprietary)
27. Lawrence Radiation Laboratory Livermore, California	Lou Zevanov	X				Indication of some work done, but none reportable

* N = No Work Q = Questionnaire Sent R = Report Received V = Visited

Table I. Companies and Laboratories Contacted for Survey Data (Continued)

Company	Contact	*				Comments
		N	Q	R	V	
28. Ling-Temco-Vought Dallas, Texas	Mike Shannon			X		Not currently active in radiation effects on microcircuits
29. Litton Industries Woodland Hills, California	A. B. Kaufman				X	
30. Lockheed Missiles and Space Company Sunnyvale, California	J. W. Cecil			X		Two reports (not received)
31. Martin Company Baltimore, Maryland	Stan Harrison	X				Work done in conjunction with Johns Hopkins Applied Physics Laboratory
32. Melpar Falls Church, Virginia	Charles Feldman	X				(Refer to Hughes, No. 23)
33. Motorola Phoenix, Arizona	I. A. Lesk				X	Studying surface effects on silicon devices
34. NASA Goddard Greenbelt, Maryland	Fred Gordon	X				(Refer to Battelle, No. 8)
35. NASA Langley Hampton, Virginia	Chris Gross			X		Abstract from Battelle (BRC)
36. Northrop Ventura Ventura, California	George Messenger				X	Currently working on programs for RADC and U. S. Signal Corps
37. Nortronics Redondo Beach, California	B. T. Ahlport	X				

* N = No Work Q = Questionnaire Sent R = Report Received V = Visited

Table I. Companies and Laboratories Contacted for Survey Data (Continued)

Company	Contact	*				Comments
		N	Q	R	V	
38. Pacific Semiconductors (TRW) Lawndale, California	Gil Downing	X				
39. Physics International Hayward, California	Henry Rugge	X				
40. RCA Laboratories Princeton, N. J.	Andrew Holmes-Siedle		X			No reply
41. Sandia Corporation Albuquerque, N. M.	J. L. Wirth	X				Have done SPRF work for Autonetics (not released)
42. Signetics Sunnyvale, California	David Allison	X				
43. Siliconix Sunnyvale, California	Lee Evans	X				
44. Sperry Great Neck, N. Y.	Jerry Rogers			X		Not received
45. Sylvania Woburn, Massachusetts		X				
46. Texas Instruments Dallas, Texas	Gary Hanson William Carr	X				Working with Boeing and Autonetics on hardening
47. Transitron Wakefield, Massachusetts	Thomas Longo	X				Testing gates and flip-flops with 2-Mev electrons (no results to date)

* N = No Work Q = Questionnaire Sent R = Report Received V = Visited

Table I. Companies and Laboratories Contacted for Survey Data (Continued)

Company	Contact	*				Comments
		N	Q	R	V	
48. Union-Carbide Mt. View, California	Mr. Hoerni	X				
49. U. S. Army Electronics Laboratory Ft. Monmouth, N. J.	E. T. Hunter		X			Sponsoring additional programs
50. USNRDL San Francisco, California	Harry Zagorites				X	Continuing surface-effect studies on thin-film components
51. UNIVAC St. Paul, Minnesota	A. J. Khambata				X	Unreported in-house program
52. Westinghouse Newbury Park, California	D. A. Deardorf	X				
53. White Sands Missile Range White Sands, N.M.	Ray Elder		X			(Refer to U. S. Army Electronics Laboratory, No. 49)

* N = No Work Q = Questionnaire Sent R = Report Received V = Visited

SECTION II

PERSPECTIVE

The principal reasons for conducting radiation-effect studies on microelectronics are to determine the system vulnerability and to develop hardened systems. As a result most of the radiation-effect data that exist on microcircuits have been obtained for particular systems; moreover, most of the data pertains to the behavior of particular microcircuits and may be termed "piece-part" data. These data were then used to estimate system responses. Results on these piece-parts may also be used to select circuits on the basis of minimum radiation response.

A second class of data, which exists in much less abundance, has long-range significance. This may be termed "basic studies" data. These data give greater insight into the response mechanisms and provide the circuit designer with the necessary information to design harder circuits.

Testing has been done that simulates three types of radiation environment: ionizing radiation, neutron radiation, and steady-state ionizing radiation. The first radiation environment, the ionizing radiation pulse from a nuclear weapon, has been simulated with flash X rays, linear-accelerator, electrons, and bremsstrahlung generated by electrons. The dosimetry was measured in almost as many different ways as there were laboratories performing the measurement but resulted in a measurement of either the exposure (in roentgens) or the absorbed dose (in rads). The majority of experimenters preferred to measure absorbed dose because the results can be interpreted independently of the radiation environment, which is not possible when only exposure information is given. A danger exists, however, in using absorbed dose information, since it cannot always be measured accurately for a given device due to the proximity of foreign construction materials of different atomic numbers.

The second radiation environment, neutrons, was simulated with reactors or by photoneutrons generated from a linear-accelerator beam. The dosimetry was performed using foil activation techniques and generally was reported as a fast flux, which usually included neutrons with energies above the plutonium activation threshold of 10 kev. For well-moderated reactors, where the thermal and low-energy neutron damage cannot be ignored, lower limits on the energy threshold are used. These differences must be considered when data from different sources are compared.

The third radiation environment used was steady-state ionizing radiation, which was simulated with Co^{60} sources and standard X-ray machines. The exposure or the absorbed dose for Co^{60} was usually calculated from the activity level and exposure time based on a known geometry. The exposure from the standard X-ray machines was measured using film and thermoluminescence dosimetry techniques.

Piece-part measurements derived from the ionizing radiation pulse include transient response at the outputs of the circuit and transient current surges in the power supplies. The circuits were tested with no input or output loads, with resistive loads, with circuit loading, and with simulated circuit loading. In every case the response was related to the logic family requirements, if any, to determine the radiation level at which failure occurs. It is possible for permanent damage to occur during this type of irradiation from bulk damage, surface effects, or burnout as a result of a "latchup" condition that causes large currents to flow in the circuit for prolonged periods of time. Usually the absorbed dose in these tests is small compared to the level required to cause significant permanent damage. In a few cases, however, "latchup" has been reported that caused permanent failures. Transient response varied greatly between each type of circuit, both as to amplitude and pulse shape. The general trend was for the amplitude to increase roughly linearly with radiation level until circuit saturation was reached. In most cases logic failure occurred far in advance of the saturation point. Flip-flops will change state at the saturation radiation levels if they are not previously in the state normally existing when power is first applied. Most circuits are dose dependent for pulses less than 0.1-microsecond wide and become rate dependent as pulse widths become much greater than this, depending on the effective carrier lifetimes in the circuit material. The outputs of all circuits are at low voltage levels during the irradiation if the radiation level is sufficiently high; however, some DTL and TTL circuits experience an increase in the output voltage level during irradiation at moderate radiation levels. Their output voltage level during irradiation falls again as the radiation level increases.

Circuit measurements made in a neutron environment include logic level voltages and switching times. The results are consistent with transistor gain degradation in that they show a marked increase in the low-level output voltage after some threshold fluence has been reached. This rise in the 0-logic level is accompanied by an increase in rise and fall times, which can also be attributed to the transistor gain degradation. Most electrical tests were performed remotely without removing the circuits from the site of their irradiation and used a typical gate-loading configuration. Frequently the loading circuits were also irradiated. There is no evidence that integrated circuits differ from their equivalent discrete component circuits in their behavior in a neutron environment.

Measurements of circuit behavior in steady-state ionizing radiation yielded results similar to those obtained in a neutron environment.

Basic studies were usually performed on circuit components and consisted primarily of data taken in ionizing radiation. Transient measurements include primary photocurrents across junctions, secondary photocurrents in transistors, and radiation-induced shunt resistance across resistors. Models have been developed to account for the presence of substrates on the radiation response of monolithic integrated circuits. These models have been used to predict circuit response. The results indicate that the presence of a substrate junction reduces the base-collector primary photocurrent and therefore the resultant secondary photocurrent. The

substrate photocurrent, however, now appears to be the mode of failure, manifesting the same behavior as if the transistor itself were conducting. The substrate current has a similar effect on resistors, providing an alternate path for current flow around the resistor. Steady-state measurements on microcircuit transistors show effects on gain, leakage current, and junction breakdown potential that are similar to those observed on standard planar transistors.

Predictions are moderately successful. The amplitude of the circuit response can be predicted within the experimental error of measurement and reproducibility of the response for similar circuits. The failure to correctly predict the long storage times seen in some circuits indicates some refinement is needed in the models used, however.

Many workers agree that obtaining piece-part data has been over-emphasized to date and that more effort should be placed on basic studies. The primary argument is that manufacturers' modifications of circuit design and construction often invalidate previous data on the response of the circuit to radiation. Historically, however, electrical improvements of circuits have resulted in improved radiation tolerance; that is, successive generations of smaller, faster circuits and components have been harder than the old, larger, slower generations. The belief now is that the technological limits are near and, unless a major breakthrough occurs in the technology, very little still remains to be gained in radiation hardness using these approaches. Perhaps a factor of 10, more or less, can be achieved in hardening through the use of oxide isolation, compatible thin-film resistors, and fabrication techniques such as those that eliminate the substrate junction. This remains to be proved, however, and such proof is currently being sought. A more promising technique for hardening is the use of ingenious circuit design exploiting difference circuitry, perhaps, and techniques that compensate for the radiation-induced photocurrents. It may well be that the monolithic integrated circuit construction will be amenable to clever design schemes for compensation by using the currents in the parasitic junctions. Certainly more consideration will have to be given to the radiation problem in the design of circuits if failure levels much beyond the present levels are to be reached.

SECTION III

SUMMARY

All the circuits and components that have been tested and described in the abstracts contained in this report are summarized in tables II, III, and IV. These tables list, respectively, the devices tested with pulsed ionizing radiation, neutron radiation, and steady-state ionizing radiation, and summarize the information on the various testing conditions used. The tables also list the maximum radiation levels attained but do not attempt to indicate the failure thresholds observed. Information on failure thresholds is given in the abstracts that are referenced in the tables.

Considering the relatively large mass of data presented, it is somewhat surprising to observe that there are very few duplications of the devices tested by the various laboratories. Test results on duplicate devices are compared in table V. The comparisons show fair agreement considering the obvious differences in dosimetry units and also the possible differences in individual devices having the same type number.

Table II. Index of Circuits Tested With Pulsed Ionizing Radiation

Manufacturer	Circuit	Source	Dosimetry	Max. Level	Pulse Width (μsec)	Measurement	Abstract No.
ACT Laboratories	Polyintegrated circuits	25- to 30-Mev electrons	SEM, calorimeter	200 rads	0.1	Output voltage Pwr sup cur.	19
	Resistor	25- to 30-Mev electrons	SEM, calorimeter	10^4 rads	0.1 to 4.5	ΔI	18
American Bosch-Arma	Word selector 1	25- to 30-Mev electrons	SEM, calorimeter	1.2×10^4 rads	0.1 to 4.5	Output current	16
	Word selector 2	25- to 30-Mev electrons	SEM, calorimeter	1.2×10^4 rads	0.1 to 4.5	Output current	16
	Prime	25- to 30-Mev electrons	SEM, calorimeter	1.2×10^4 rads	0.1 to 4.5	Output current	16
	Micro A flip-flop	25- to 30-Mev electrons	SEM, calorimeter	1.2×10^4 rads	0.1 to 4.5	Output current	16
	Micro B flip-flop	25- to 30-Mev electrons	SEM, calorimeter	1.2×10^4 rads	0.1 to 4.5	Output current	16
Autonetics GCML	Diffused resistor	600-kv flash X ray	Film	8×10^6 rad/sec	0.12	ΔI	2
	Polycrystalline resistor	600-kv flash X ray	Film	8×10^6 rad/sec	0.12	ΔI	2
	Thin-film resistor	600-kv flash X ray	Film	8×10^6 rad/sec	0.12	ΔI	2

Table II. Index of Circuits Tested With Pulsed Ionizing Radiation (Continued)

Manufacturer	Circuit	Source	Dosimetry	Max. Level	Pulse Width (μsec)	Measurement	Abstract No.
Autonetics (Continued)	CPC resistor	600-kv flash X ray	Film	8×10^6 rad/sec	0.12	ΔI	2
Fairchild	μL900	10-Mev electrons	Si diode, glass rods	4×10^9 rad/sec	0.2	Output voltage	8
		10-Mev electrons	Si diode, glass rods	2×10^9 rad/sec	0.2	Pwr sup cur.	10
	μL902	10-Mev electrons	Si diode, glass rods	2×10^9 rad/sec	0.2	Pwr sup cur.	8
		10-Mev brem.	Faraday cup, glass rods	5×10^8 R/sec	1	Output voltage	23
		600-kv flash X ray	Photodiode Si photo-conductivity	5×10^6 R/sec	0.2	Output voltage	31
	μL903	10-Mev electrons	Si diode, glass rods	4×10^9 rad/sec	0.2	Output voltage Pwr sup cur.	8
		10-Mev brem.	Faraday cup, glass rods	5×10^8 R/sec	1	Output voltage	23
	G	600-kv flash X ray	Photodiode Si photo-conductivity	5×10^6 R/sec	0.2	Output voltage	31
	μL904	10-Mev electrons	Si diode, glass rods	4×10^9 rad/sec	0.2	Output voltage Pwr sup cur.	8

Table II. Index of Circuits Tested With Pulsed Ionizing Radiation (Continued)

Manufacturer	Circuit	Source	Dosimetry	Max. Level	Pulse Width (μsec)	Measurement	Abstract No.
Fairchild (Continued)	μL906	10-Mev electrons	Si diode, glass rods	4×10^9 rad/sec	0.2	Output voltage Pwr sup cur.	8
	μL914	SPRF gamma ray	Glass rods	6×10^7 rad(C)/sec	50	Output current voltage	12
	MwμL910	10-Mev electrons	Si diode, glass rods	4×10^9 rad/sec	0.2	Output voltage Pwr sup cur.	8
	DTμL931	150-kv flash X ray	---	2×10^9 R/sec	20 nsec	Logic change	28
	μC101	10-Mev electrons	Si diode, glass rods	4×10^9 rad/sec	0.2	Output voltage Pwr sup cur.	8
	μC108	10-Mev electrons	Si diode, glass rods	3×10^{10} rad/sec	50 nsec	Output voltage Pwr sup cur.	9
	μC110	10-Mev electrons	Si diode, glass rods	3×10^{10} rad/sec	50 nsec	Output voltage Pwr sup cur.	9
	μC111	10-Mev electrons	Si diode, glass rods	3×10^{10} rad/sec	50 nsec	Output voltage Pwr sup cur.	9
	μET-1	10-Mev brem.	Faraday cup, glass rods	5×10^7 R/sec	1	ΔI	23
	μET-2	10-Mev brem.	Faraday cup, glass rods	5×10^7 R/sec	1	ΔI	23
	μER-2	10-Mev brem.	Faraday cup, glass rods	5×10^7 R/sec	1	ΔI	23

Table II. Index of Circuits Tested With Pulsed Ionizing Radiation (Continued)

Manufacturer	Circuit	Source	Dosimetry	Max. Level	Pulse Width (μsec)	Measurement	Abstract No.
Fairchild (Continued)	μER-1	600-kv flash X ray	Film	8×10^6 rad/sec	0.12	ΔI	2
	LINC circuits	10-Mev brem.	Faraday cup, glass rods	10^8 R/sec	1	Output voltage	26
General Electric	Low-level switch	25- to 30-Mev	SEM, calorimeter	500 rads	0.1	Pwr sup cur.	15
General Micro-electronics	LINC circuits	10-Mev brem.	Faraday cup, glass rods	10^8 R/sec	1	Output voltage	26
	A	10-Mev electrons	Si diode, glass rods	4×10^9 rad/sec	0.2	Output voltage Pwr sup cur.	8
	B						
	D_2						
	G						
	R						
Honeywell	MHM3001	10-Mev electrons	Si diode, glass rods	4×10^9 rad/sec	0.2	Output voltage Pwr sup cur.	8
	MHM3101						
	MHM3201						

Table II. Index of Circuits Tested With Pulsed Ionizing Radiation (Continued)

Manufacturer	Circuit	Source	Dosimetry	Max. Level	Pulse Width (μsec)	Measurement	Abstract No.
International Resistor Corporation	HD903	10-Mev electrons	Si diode, glass rods	3×10^9 rad/sec	0.2	Output voltage Pwr sup cur.	10
Melpar	MM1001	10-Mev electrons	Si diode, glass rods	4×10^9 rad/sec	0.2	Output voltage Pwr sup cur.	8
	Thin-film bi-stable network	6-Mev electrons and 10-Mev brem.	Faraday cup, glass rods	5×10^8 rad/sec(γ) 10^{10} rad/sec(e^-)	1	Output voltage	23
	Thin-film 4-kc oscillator	6-Mev electrons and 10-Mev brem.	Faraday cup, glass rods	5×10^8 rad/sec(γ) 10^{10} rad/sec(e^-)	1	Output voltage	23
Motorola	LINC	10-Mev brem.	Faraday cup, glass rods	10^8 R/sec	1	Output voltage	26
	Dual four-input TTL gate	25- to 30-Mev electrons	SEM, calorimeter	10^4 rads	0.1 to 4.5	Pwr sup cur.	18
	Logic flip-flop	25- to 30-Mev electrons	SEM, calorimeter	3×10^4 rads	0.1 to 4.5	Pwr sup cur.	17
	One-shot multivibrator	25- to 30-Mev electrons	SEM, calorimeter	3×10^4 rads	0.1 to 4.5	Pwr sup cur.	17
	One-shot multivibrator	25- to 30-Mev electrons	SEM, calorimeter	10^4 rads	0.1 to 4.5	Pwr sup cur.	18
	MC302G	10-Mev electrons	Si diode, glass rods	4×10^9 rad/sec	0.2	Output voltage Pwr sup cur.	8

Table II. Index of Circuits Tested With Pulsed Ionizing Radiation (Continued)

Manufacturer	Circuit	Source	Dosimetry	Max. Level	Pulse Width (μsec)	Measurement	Abstract No.
Motorola (Continued)	MC303G	10-Mev electrons	Si diode, glass rods	4×10^9 rad/sec	0.2	Output voltage Pwr sup cur.	8
	MC304G			4×10^9 rad/sec			8
	MC306G			4×10^9 rad/sec			8
	MC356G			2×10^9 rad/sec			10
	MC1110			4×10^9 rad/sec			8
Pacific Semiconductor (TRW)	PCD011	10-Mev electrons	Si diode, glass rods	4×10^9 rad/sec	0.2	Output voltage Pwr sup cur.	8
	PCF101						8
	PCG102						8
	PCS101						8
Philco	μ7006	10-Mev brem.	Faraday cup, glass rods	5×10^8 R/sec	1	Output voltage	23
	LINC						26
Radio Corporation of America	34769	25- to 30-Mev electrons	SEM, calorimeter	200 rads	0.1	Output voltage Pwr sup cur.	19

Table II. Index of Circuits Tested With Pulsed Ionizing Radiation (Continued)

Manufacturer	Circuit	Source	Dosimetry	Max. Level	Pulse Width (μsec)	Measurement	Abstract No.
Raytheon	RC103	10-Mev electrons	Si diode, glass rods	4×10^{9} rad/sec	0.2	Output voltage Pwr sup cur.	8
Signetics	SE101G	10-Mev electrons	Si diode, glass rods	3×10^{10} rad/sec	50 nsec	Output voltage Pwr sup cur.	9
	SE102G	10-Mev electrons	Si diode, glass rods	4×10^{9} rad/sec	0.2	Output voltage Pwr sup cur.	8
	SE102K	10-Mev brem.	Faraday cup, glass rods	5×10^{8} R/sec	1	Output voltage	23
	SE105G	10-Mev electrons	Si diode, glass rods	3×10^{10} rad/sec	50 nsec	Output voltage Pwr sup cur.	9
	SE110G	10-Mev electrons	Si diode, glass rods	4×10^{9} rad/sec	0.2	Output voltage Pwr sup cur.	8
	SE115	600-kv flash X ray	Photodiode, Si photo-conductivity	5×10^{6} R/sec	0.2	Output voltage	31
	SE121T	600-kv flash X ray	Photodiode, Si photo-conductivity	5×10^{6} R/sec	0.2	Output voltage	31
	SE124G	10-Mev electrons	Si diode, glass rods	4×10^{9} rad/sec	0.2	Output voltage Pwr sup cur.	8

Table II. Index of Circuits Tested With Pulsed Ionizing Radiation (Continued)

Manufacturer	Circuit	Source	Dosimetry	Max. Level	Pulse Width (μsec)	Measurement	Abstract No.
Signetics (Continued)	SE124G	10-Mev electrons	Si diode, glass rods	3×10^{9} rad/sec	50 nsec	Output voltage Pwr sup cur.	9
	SE160G	10-Mev electrons	Si diode, glass rods	4×10^{9} rad/sec	0.2	Output voltage Pwr sup cur.	8
	SE160G	10-Mev electrons	Si diode, glass rods	3×10^{10} rad/sec	50 nsec	Output voltage Pwr sup cur.	9
	CS701	10-Mev electrons	Si diode, glass rods	3×10^{10} rad/sec	50 nsec	Output voltage Pwr sup cur.	9
	LINC	10-Mev brem.	Faraday cup, glass rods	10^{8} R/sec	1	Output voltage	26
	C1050	10-Mev electrons	Si diode, glass rods	3×10^{10} rad/sec	50 nsec	Output voltage Pwr sup cur.	9
	C1052	↑	↑	↑	↑	↑	↑
	C1053G	↑	↑	↑	↑	↑	↑
	C1054	↑	↑	↑	↑	↑	↑
	C1055	↑	↑	↑	↑	↑	↑
	C1063	↑	↑	↑	↑	↑	↑
	C1065	↑	↑	↑	↑	↑	↑
	C1073	10-Mev electrons	Si diode, glass rods	3×10^{10} rad/sec	50 nsec	Output voltage Pwr sup cur.	9

Table II. Index of Circuits Tested With Pulsed Ionizing Radiation (Continued)

Manufacturer	Circuit	Source	Dosimetry	Max. Level	Pulse Width (μsec)	Measurement	Abstract No.
Signetics (Continued)	C5051G	10-Mev electrons	Si diode, glass rods	3×10^{10} rad/sec	50 nsec	Output voltage Pwr sup cur.	9
	PF800T	10-Mev brem.	Faraday cup, glass rods	5×10^{8} R/sec	1	ΔI_c	23
	PF801T	10-Mev brem.	Faraday cup, glass rods	5×10^{8} R/sec	1	ΔI_c	23
	PF860T	600-kv flash X ray	Film	8×10^{6} rad/sec	0.12	ΔI	2
	PF861T	600-kv flash X ray	Film	8×10^{6} rad/sec	0.12	ΔI	2
	PF861T	600-kv flash X ray	Photodiode, Si photo-conductivity	5×10^{6} R/sec	0.2	ΔI	31
	PF861T	25- to 30-Mev electrons	SEM, calorimeter	10^{3} rads	0.1	ΔI	18
Siliconix	A01A	10-Mev electrons	Si diode, glass rods	4×10^{9} rad/sec	0.2	Output voltage Pwr sup cur.	8
Sperry	113K3	10-Mev electrons	Si diode, glass rods	3×10^{10} rad/sec	50 nsec	Output voltage Pwr sup cur.	9
Sylvania	SNG3	10-Mev electrons	Si diode, glass rods	4×10^{9} rad/sec	0.2	Output voltage Pwr sup cur.	8

Table II. Index of Circuits Tested With Pulsed Ionizing Radiation (Continued)

Manufacturer	Circuit	Source	Dosimetry	Max. Level	Pulse Width (μsec)	Measurement	Abstract No.
Sylvania (Continued)	SNG5A	10-Mev electrons	Si diode, glass rods	3×10^{10} rad/sec	50 nsec	Output voltage Pwr sup cur.	9
	SNG7	10-Mev electrons	Si diode, glass rods	4×10^{9} rad/sec	0.2	Output voltage Pwr sup cur.	8
	SFF2A	25- to 30-Mev electrons	SEM, calorimeter	1.2×10^{4} rad	0.1 to 4.5	Output current	16
	LINC	10-Mev brem.	Faraday cup, glass rods	10^{8} R/sec	1	Output voltage	26
Texas Instruments	LINC	10-Mev brem.	Faraday cup, glass rods	10^{8} R/sec	1	Output voltage	26
	SN336	25- to 30-Mev electrons	SEM, calorimeter	500 rads	0.1	Pwr sup cur.	15
				3×10^{4} rads	0.1 to 4.5		17
				10^{4} rads	0.1 to 4.5		18
	SN337			500 rads	0.1		15
				3×10^{4} rads	0.1 to 4.5	Pwr sup cur.	17
				200 rads	0.1	Output voltage Pwr sup cur.	19
	SN338	25- to 30-Mev electrons	SEM, calorimeter	500 rads	0.1	Pwr sup cur.	15

Table II. Index of Circuits Tested With Pulsed Ionizing Radiation (Continued)

Manufacturer	Circuit	Source	Dosimetry	Max. Level	Pulse Width (μsec)	Measurement	Abstract No.
Texas Instruments (Continued)	SN340	25- to 30-Mev electrons	SEM, calorimeter	500 rads	0.1	Pwr sup cur.	15
				$3x10^4$ rads	0.1 to 4.5		17
	SN341			$3x10^4$ rads	0.1 to 4.5		17
				500 rads	0.1		15
	SN342			500 rads	0.1		15
				$3x10^4$ rads	0.1 to 4.5		17
				10^4 rads	0.1 to 4.5		18
	SN343			500 rads	0.1		15
				$3x10^4$	0.1 to 4.5		17
	SN344			500 rads	0.1	Pwr sup cur.	15
				200 rads	0.1	Output voltage Pwr sup cur.	19
	SN345			200 rads	0.1	Output voltage Pwr sup cur.	19
				500 rads	0.1	Pwr sup cur.	15
				$3x10^4$ rads	0.1 to 4.5	Pwr sup cur.	17
		25- to 30-Mev electrons	SEM, calorimeter	10^4 rads	0.1 to 4.5	Pwr sup cur.	18

Table II. Index of Circuits Tested With Pulsed Ionizing Radiation (Continued)

Manufacturer	Circuit	Source	Dosimetry	Max. Level	Pulse Width (μsec)	Measurement	Abstract No.
Texas Instruments (Continued)	SN346	25- to 30-Mev electrons	SEM, calorimeter	500 rads	0.1	Pwr sup cur.	15
				3×10^4 rads	0.1 to 4.5		17
	SN347			3×10^4 rads	0.1 to 4.5		17
				10^4 rads	0.1 to 4.5		18
				500 rads	0.1		15
	SN348			500 rads	0.1	Pwr sup cur.	15
				200 rads	0.1	Output voltage Pwr sup cur.	19
				3×10^4 rads	0.1 to 4.5	Pwr sup cur.	17
	SN349			3×10^4 rads	0.1 to 4.5		17
				500 rads	0.1		15
	SN350			500 rads	0.1		15
	SN351			500 rads	0.1		15
				3×10^4 rads	0.1 to 4.5		17
				10^4 rads	0.1 to 4.5		18
	SN352			500 rads	0.1		15
	SN354	25- to 30-Mev electrons	SEM, calorimeter	500 rads	0.1	Pwr sup cur.	15

Table II. Index of Circuits Tested With Pulsed Ionizing Radiation (Continued)

Manufacturer	Circuit	Source	Dosimetry	Max. Level	Pulse Width (μsec)	Measurement	Abstract No.
Texas Instruments (Continued)	SN354 (Continued)	25- to 30-Mev electrons	SEM, calorimeter	200 rads	0.1	Output voltage Pwr sup cur.	19
				3×10^4 rads	0.1 to 4.5	Pwr sup cur.	17
	SN355			3×10^4 rads	0.1 to 4.5	Pwr sup cur.	17
				10^4 rads	0.1 to 4.5	Pwr sup cur.	18
		25- to 30-Mev electrons	SEM, calorimeter	500 rads	0.1	Pwr sup cur.	15
	SN510	10-Mev brem.	Faraday cup, glass rods	5×10^8 R/sec	1	Output voltage	23
		10-Mev electrons	Si diode, glass rods	4×10^9 rad/sec	0.2	Output voltage	8
	SN514	10-Mev electrons	Si diode, glass rods	4×10^9 rad/sec	0.2	Output voltage	8
	SN522	10-Mev electrons	Si diode, glass rods	4×10^9 rad/sec	0.2	Output voltage	8
	SN530	25- to 30-Mev electrons	SEM, calorimeter	1.2×10^4 rads	0.1 to 4.5	Output current	16
	Series 51 transistors	480-kv flash X ray	Ion chamber	5×10^6 R/sec	0.2	I_{pp}, I_{sp}	7
	Series 51 capacitors	480-kv flash X ray	Ion chamber	5×10^6 R/sec	0.2	I_{pp}	7

Table II. Index of Circuits Tested With Pulsed Ionizing Radiation (Continued)

Manufacturer	Circuit	Source	Dosimetry	Max. Level	Pulse Width (μsec)	Measurement	Abstract No.
Transitron	Three-input gate	10-Mev electrons	Si diode, glass rods	4×10^9 rad/sec	0.2	Output voltage Pwr sup cur.	8
VARO	8201	10-Mev electrons	Si diode, glass rods	3×10^9 rad/sec	0.2	Output voltage Pwr sup cur.	20
Westinghouse	W2601	25- to 30-Mev electrons	SEM, calorimeter	500 rads	0.1	Pwr sup cur.	15
				3×10^4 rads	0.1 to 4.5	Pwr sup cur.	17
				200 rads	0.1	Output voltage Pwr sup cur.	19
	W2602			200 rads	0.1	Output voltage Pwr sup cur.	19
				500 rads	0.1	Pwr sup cur.	15
				3×10^4 rads	0.1 to 4.5		17
	W2603			3×10^4 rads	0.1 to 4.5		17
				500 rads	0.1		15
	W2604			500 rads	0.1		15
				3×10^4 rads	0.1 to 4.5		17
		25- to 30-Mev electrons	SEM, calorimeter	10^4	0.1 to 4.5	Pwr sup cur.	18

Table II. Index of Circuits Tested With Pulsed Ionizing Radiation (Continued)

Manufacturer	Circuit	Source	Dosimetry	Max. Level	Pulse Width (μsec)	Measurement	Abstract No.
Westinghouse (Continued)	WS130	10-Mev electrons	Si diode, glass rods	3×10^{10} rad/sec	50 nsec	Output voltage Pwr sup. cur.	9
	WS131						
	WS133Q						
	WS135						
	WS208Q						
	WS268Q						
	WS269Q						
	WS270Q						
	WS271Q						
	WS272Q						
	WS8149	10-Mev electrons	Si diode, glass rods	3×10^{10} rad/sec	50 nsec	Output voltage Pwr sup cur.	9
	Matrix switch	25- to 30-Mev electrons	SEM, calorimeter	500 rads	0.1	Pwr sup cur.	15
	WM201	10-Mev electrons	Si diode, glass rods	4×10^{9} rad/sec	0.2	Output voltage Pwr sup cur.	8
	WM202	10-Mev electrons	Si diode, glass rods	4×10^{9} rad/sec	0.2	Output voltage Pwr sup cur.	8

Table II. Index of Circuits Tested With Pulsed Ionizing Radiation (Continued)

Manufacturer	Circuit	Source	Dosimetry	Max. Level	Pulse Width (μsec)	Measurement	Abstract No.
Westinghouse (Continued)	W914	25- to 30-Mev electrons	SEM, calorimeter	500 rads	0.1	Pwr sup cur.	15
				$3x10^4$ rads	0.1 to 4.5		17
	W915			500 rads	0.1		15
	W916			500 rads	0.1		15
				$3x10^4$ rads	0.1 to 4.5		17
	W917			$3x10^4$ rads	0.1 to 4.5		17
				500 rads	0.1		15
	W921			$3x10^4$ rads	0.1 to 4.5		17
	W923	25- to 30-Mev electrons	SEM, calorimeter	500 rads	0.1	Pwr sup cur.	15
	W2101	600-kv flash X ray	Photodiode, Si photo-conductivity	$5x10^6$ R/sec	0.2	Output voltage	31
	W2102	600-kv flash X ray	Photodiode, Si photo-conductivity	$5x10^6$ R/sec	0.2	Output voltage	31
	Low-level switch	25- to 30-Mev electrons	SEM, calorimeter	500 rads	0.1	Pwr sup cur.	15
		25- to 30-Mev electrons	SEM, calorimeter	$3x10^4$ rads	0.1 to 4.5	Pwr sup cur.	17

Table II. Index of Circuits Tested With Pulsed Ionizing Radiation (Continued)

Manufacturer	Circuit	Source	Dosimetry	Max. Level	Pulse Width (μsec)	Measurement	Abstract No.
Westinghouse (Continued)	Output driver	25- to 30-Mev electrons	SEM, calorimeter	500 rads	0.1	Pwr sup cur.	15
	Read pre-amplifier	↕	↕	500 rads	0.1	↕	15
				10^4 rads	0.1 to 4.5		17
	Write switch			10^4 rads	0.1 to 4.5		17
		25- to 30-Mev electrons	SEM, calorimeter	500 rads	0.1	Pwr sup cur.	15

Table III. Index of Circuits Tested With Neutron Radiation

Manufacturer	Circuit	Source	Max. Level (n/cm^2)	E_n >	Measurement	Abstract No.
American Bosch-Arma	Word selector 1	TRIGA - GA	$3x10^{14}$	10 kev	Logic levels	16
	Word selector 2		$5x10^{14}$			
	Prime		$3x10^{14}$			
	Micro A flip-flop		$3x10^{14}$			
Fairchild	μL903	25-Mev photoneutrons	10^{15}	10 kev	Logic levels, Switching times	8
	μC108		$3x10^{14}$			9
	μC110		$3x10^{14}$			9
	μC111		$3x10^{14}$			9
	μA702		$4x10^{14}$			9
	DTμL931	25-Mev photoneutrons	$4x10^{14}$		Logic levels, Switching times	9
	μL914	Penn. State U. reactor	$4.1x10^{14}$		Logic levels	11
	G	TRIGA at Northrop	10^{15}	10 kev	Logic levels	31
		U. of Florida reactor	10^{15}	0.4 ev	Logic levels	20
		UCLA reactor	$2x10^{15}$	0.4 ev	Logic levels, Switching times	14
	B	UCLA reactor	$2x10^{15}$	0.4 ev	Logic levels, Switching times	14

Table III. Index of Circuits Tested With Neutron Radiation (Continued)

Manufacturer	Circuit	Source	Max. Level (n/cm^2)	$E_n >$	Measurement	Abstract No.
Fairchild (Continued)	H	UCLA reactor	$2x10^{15}$	0.4 ev	Logic levels, Switching times	14
	S	UCLA reactor	$2x10^{15}$	0.4 ev	Logic levels, Switching times	14
	LINC	GA Mark I	$1.2x10^{14}$	10 kev	Logic levels	26
	MWμL910	GA Mark I	$1.2x10^{14}$	10 kev	Logic levels	26
	MWμL913	GA Mark I	$1.2x10^{14}$	10 kev	Logic levels	26
	μC103	U. of Florida reactor	$2.3x10^{13}$	3 Mev	Logic levels, Switching times	21
		U. of Florida reactor	$3x10^{14}$	3 Mev	Logic levels, Switching times	22
	μL900	U. of Florida reactor	$3x10^{14}$	3 Mev	Logic levels, Switching times	22
		U. of Florida reactor	$2.3x10^{13}$	3 Mev	Logic levels, Switching times	21
General Electric	P324	UCLA reactor	$2x10^{15}$	0.4 ev	Logic levels, Switching times	14
	P325					

Table III. Index of Circuits Tested With Neutron Radiation (Continued)

Manufacturer	Circuit	Source	Max. Level (n/cm^2)	$E_n >$	Measurement	Abstract No.
General Microelectronics	LINC Mw logic 913	GA Mark I	1.2×10^{14}	10 kev	Logic levels	26
Honeywell	MHM3001	25-Mev photoneutrons	10^{15}	10 kev	Logic levels, Switching times	8
	ES1001	U. of Florida reactor	3×10^{14}	3 Mev	Logic levels, Switching times	22
	Type K flip-flop	U. of Florida reactor	2.3×10^{13}	3 Mev	Logic levels, Switching times	21
	Type S flip-flop	U. of Florida reactor	2.3×10^{13}	3 Mev	Logic levels, Switching times	21
Motorola	SC340	U. of Florida reactor	2.3×10^{13}	3 Mev	Logic levels, Switching times	21
	LINC	GA Mark I	1.2×10^{14}	10 kev	Logic levels	26
	MC306G	SPRF	4×10^{14}	10 kev	Logic levels	11
		UCLA reactor	2×10^{15}	0.4 ev	Logic levels, Switching times	14
	MC304G	25-Mev photoneutrons	10^{15}	10 kev	Logic levels, Switching times	8
	XC201	25-Mev photoneutrons	4×10^{14}	10 kev	Logic levels, Switching times	9

Table III. Index of Circuits Tested With Neutron Radiation (Continued)

Manufacturer	Circuit	Source	Max. Level (n/cm^2)	$E_n >$	Measurement	Abstract No.
Norden	Differential amplifier	25-Mev photoneutrons	$3x10^{14}$	10 kev	Logic levels, Switching times	9
Pacific Semiconductor (TRW)	Binary counter	UCLA reactor	$2x10^{15}$	0.4 ev	Logic levels, Switching times	14
	Three-input gate					
Philco	LINC Mw logic 911	GA Mark I	$1.2x10^{14}$	10 kev	Logic levels	26
Radio Corporation of America	34769	TRIGA - GA	$3.5x10^{12}$	10 kev	Gain, Z_{in}	3
Raytheon	RC103	25-Mev photoneutrons	10^{15}	10 kev	Logic levels, Switching times	8
Signetics	SE102	25-Mev photoneutrons	10^{15}	10 kev	Logic levels, Switching times	8
		TRIGA at Northrop	10^{15}	10 kev	Logic levels	31
	SE100T	U. of Florida reactor	10^{15}	0.4 ev	Logic levels	20
		UCLA reactor	$2x10^{15}$	0.4 ev	Logic levels, Switching times	14
	SE101G	25-Mev photoneutrons	$3x10^{14}$	10 kev	Logic levels, Switching times	9

Table III. Index of Circuits Tested With Neutron Radiation (Continued)

Manufacturer	Circuit	Source	Max. Level (n/cm^2)	$E_n >$	Measurement	Abstract No.
Signetics (Continued)	SE105G	25-Mev photoneutrons	$3x10^{14}$	10 kev	Logic levels, Switching times	9
	SE124G	25-Mev photoneutrons	$3x10^{14}$	10 kev	Logic levels, Switching times	9
	SE124K	U. of Florida reactor	$2.3x10^{13}$	3 Mev	Logic levels, Switching times	21
		U. of Florida reactor	$3x10^{14}$	3 Mev	Logic levels, Switching times	22
		TRIGA at Northrop	10^{15}	10 kev	Logic levels	31
	SE120	UCLA reactor	$2x10^{15}$	0.4 ev	Logic levels, Switching times	14
	LINC	GA Mark I	$1.2x10^{14}$	10 kev	Logic levels	26
	CS701	25-Mev photoneutrons	$3x10^{14}$	↕	Logic levels, Switching times	9
	SE160G	↕	↕	↕	↕	↕
	C1050	↕	↕	↕	↕	↕
	C1052	↕	↕	↕	↕	↕
	C1053G	↕	↕	↕	↕	↕
	C1054	25-Mev photoneutrons	$3x10^{14}$	10 kev	Logic levels, Switching times	9

Table III. Index of Circuits Tested With Neutron Radiation (Continued)

Manufacturer	Circuit	Source	Max. Level (n/cm^2)	E_n >	Measurement	Abstract No.
Signetics (Continued)	C1055	25-Mev photoneutrons	$3x10^{14}$	10 kev	Logic levels, Switching times	9
	C1063					
	C1065					
	C1073					
	C5051G	25-Mev photoneutrons	$3x10^{14}$	10 kev	Logic levels, Switching times	9
Sperry	113K3	25-Mev photoneutrons	$3x10^{14}$	10 kev	Logic levels, Switching times	9
Sylvania	SNG3	TRIGA - GA	$3x10^{14}$	10 kev	Logic levels	1
	SFF2A	TRIGA - GA	10^{15}	10 kev	Logic levels	16
	SNG4	U. of Florida reactor	$2.3x10^{13}$	3 Mev	Logic levels, Switching times	21
	LINC	GA Mark I	$1.2x10^{14}$	10 kev	Logic levels	26
	SFF3A	25-Mev photoneutrons	$4x10^{14}$	10 kev	Logic levels, Switching times	9
	SNG5A	25-Mev photoneutrons	$3x10^{14}$	10 kev	Logic levels, Switching times	9
	SFF13	25-Mev photoneutrons	$4x10^{14}$	10 kev	Logic levels, Switching times	9

Table III. Index of Circuits Tested With Neutron Radiation (Continued)

Manufacturer	Circuit	Source	Max. Level (n/cm^2)	$E_n >$	Measurement	Abstract No.
Sylvania (Continued)	M0057	UCLA reactor	2×10^{15}	0.4 ev	Logic levels, Switching times	14
	M0043	UCLA reactor	2×10^{15}	0.4 ev	Logic levels, Switching times	14
Texas Instruments	SN349	TRIGA - GA	3.5×10^{12}	10 kev	Gain, Z_{in}	3
	SN350	↕	↕	↕	↕	↕
	SN351					
	SN352					
	SN354					
	SN355	TRIGA - GA	3.5×10^{12}	10 kev	Gain, Z_{in}	3
	SN510	25-Mev photoneutrons	10^{15}	10 kev	Logic levels	8
		SPRF	3.5×10^{12}	3 Mev	Logic levels	23
		UCLA reactor	2×10^{15}	0.4 ev	Logic levels, Switching times	13
	SN511	UCLA reactor	2×10^{15}	0.4 ev	Logic levels, Switching times	13
		---	5.4×10^{14}	---	Logic level	27
	SN512	UCLA reactor	2×10^{15}	0.4 ev	Logic levels, Switching times	13

Table III. Index of Circuits Tested With Neutron Radiation (Continued)

Manufacturer	Circuit	Source	Max. Level (n/cm^2)	$E_n >$	Measurement	Abstract No.
Texas Instruments (Continued)	SN514	UCLA reactor	2×10^{15}	0.4 ev	Logic levels, Switching times	13
		SPRF	8.5×10^{12}	3 Mev	Logic levels	23
	SN522	---	5.4×10^{14}	---	Logic levels	27
	SN533	U. of Florida reactor	2.3×10^{13}	3 Mev	Logic levels, Switching times	21
	SN1118	U. of Florida reactor	3×10^{14}	3 Mev	Logic levels, Switching times	22
	SN1119	U. of Florida reactor	3×10^{14}	3 Mev	Logic levels, Switching times	22
	LINC	GA Mark I	1.2×10^{14}	10 kev	Logic levels	26
Transitron	TNG3211F	25-Mev photoneutrons	4×10^{14}	10 kev	Logic levels, Switching times	9
Westinghouse	WS130	25-Mev photoneutrons	3×10^{14}	10 kev	Logic levels, Switching times	9
	WS131					
	WS133Q					
	WS135					
	WS208Q					

Table III. Index of Circuits Tested With Neutron Radiation (Continued)

Manufacturer	Circuit	Source	Max. Level (n/cm^2)	$E_n >$	Measurement	Abstract No.
Westinghouse (Continued)	WS268Q WS269Q WS270Q WS271Q WS272Q WS8149	25-Mev photoneutrons	$3x10^{14}$	10 kev	Logic levels, Switching times	9

Table IV. Index of Circuits Tested With Steady-State Ionizing Radiation

Manufacturer	Circuits	Radiation Source	Dosimetry	Max. Dose	Measurement	Abstract No.
Amelco	G11001	X ray	Film, thermo-luminescence	3.7×10^7 R	h_{fe}, V_{SAT} $V_{breakdown}$	6
Fairchild	F	Co^{60}	Calculated	2×10^8 rads	I_{CBO}, gain	5
General Microelectronics	D412	X ray	Film, thermo-luminescence	3.7×10^7 R	h_{fe}, V_{SAT} $V_{breakdown}$	6
Melpar	Thin-film active	Co^{60}	Calculated	1.6×10^6 R	I_D, I_{GSS}	34
Motorola	Transistors	Co^{60}	Calculated	3.5×10^6 R	Gain, I_{CBO}	29
Raytheon	RC103	X ray	Film, thermo-luminescence	3.7×10^7 R	h_{fe}, V_{SAT} $V_{breakdown}$	6
Texas Instruments	SN310	Co^{60}	Calculated	2×10^8 rads	I_{CBO}, gain	5
	SN511A	Co^{60}	Calculated	2.4×10^7 rads	Logic levels, Switching times	24
		200-kev brem. 6-Mev electrons 22-Mev protons	---	---- 5.5×10^{14} e^-/cm^2 10^{13} p/cm^2	---	32
	SN513A	Co^{60}	Calculated	2.4×10^7 rads	Logic levels, Switching times	24

Table IV. Index of Circuits Tested With Steady-State Ionizing Radiation (Continued)

Manufacturer	Circuits	Radiation Source	Dosimetry	Max. Dose	Measurement	Abstract No.
Texas Instruments (Continued)	SN514A	Co^{60}	Calculated	2.4×10^{7} rads	Logic levels, Switching times	24
---	Transistors	22-Mev protons 40-Mev protons 128-Mev protons 440-Mev protons	---	10^{11} p/cm^2	---	30

Table V. Comparison of Data Obtained by Different Workers

Device	Radiation Failure Level	Abstract No.
Pulsed Ionizing Radiation		
Fairchild μL902	2.3×10^8 rad/sec	8
μL902	2×10^7 R/sec	23
Fairchild μL903	2 to 3×10^8 rad/sec	8
μL903	$< 10^8$ R/sec	23
Signetics SE102G	40 rads (0.2 μsec)	8
SE102K	100 roentgens (1.0 μsec)	23
Texas Instruments SN510	3 to 3.6 rads (0.2 μsec)	8
SN510	0.4 or 6 roentgens (1.0 μsec)	23
Neutron Radiation		
Texas Instruments SN510	10^{14} n/cm^2 ($E_n > 10$ kev)	8
SN510	1.8×10^{14} n/cm^2 ($E_n > 0.4$ ev)	13
SN510	3.5×10^{12} n/cm^2 ($E_n > 3$ Mev)	23

SECTION IV

ABSTRACTS

This section presents a series of 34 abstracts of unclassified documents or of data supplied through private communications. Some of these abstracts have been taken directly from the Battelle Radiation Effects Information Center file of abstracts and have been so identified.

A classified supplement, which appears under separate cover, contains similar information taken from nine classified documents.

ABSTRACT 1: AMERICAN BOSCH-ARMA CORPORATION

Laboratory Study of the Neutron Radiation Effects on Microcircuit Digital Gates, DS-64-R371-44, June 1964

Author: Bernard Gaines

The Sylvania SNG-3, TTL, NAND gate was irradiated at the General Atomic TRIGA Reactor with fluences up to 3×10^{14} n/cm^2 ($E_n > 10$ kev). Dosimetry was performed by General Atomic using activation foils. Electrical measurements were made of the grounded emitter I_C versus V_{CE} characteristics, propagation delay, input load current (a measure of the resistor value), input leakage current, "on" level of the output transistor (a measure of saturation voltage), and I_t versus V_t (a measure of the input voltage required to produce a 100-microampere collector current at the output, which is a measure of noise immunity).

No effect was measured on the resistors. Although the transistor gain had degraded appreciably (figure 1), the increase of the "on" level voltage from 0.28 to 0.35 volt over the last decade of fluence was still insufficient to cause failure (0.40 volt).

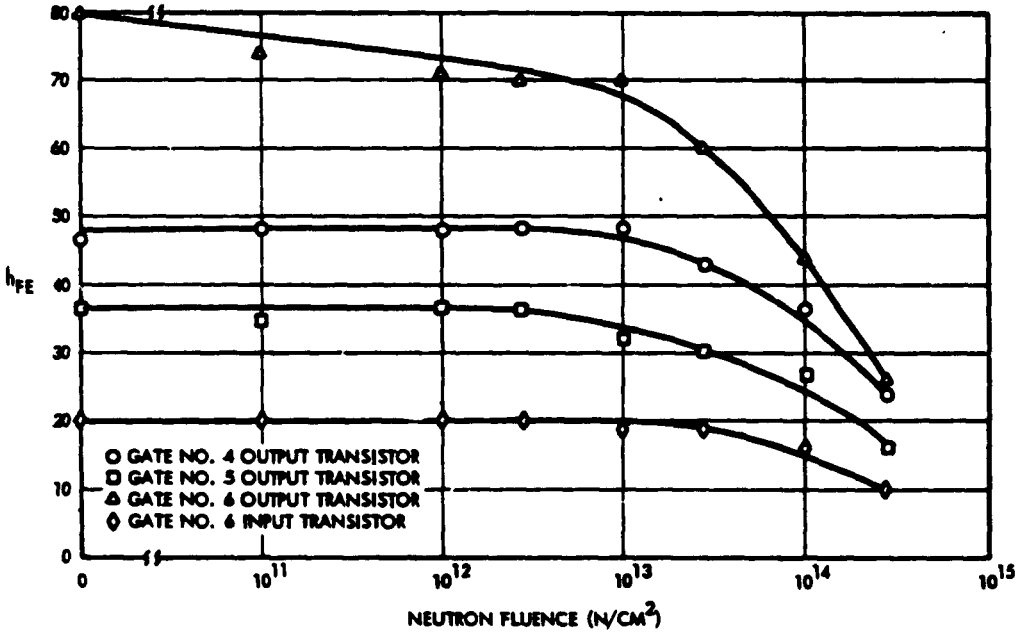

Figure 1. Transistor gain degradation under neutron irradiation for Sylvania SNG3 gate.

ABSTRACT 2: AUTONETICS

Transient Radiation Effects on Common Microelectronic Resistor Types, presented at IEEE/PTGNS Special Technical Conference on Nuclear Radiation Effects, Seattle, Washington, July 20-23, 1964

Authors: T. C. Getten, E. M. Coffin, E. E. Griffin, Jr., and A. S. Hoffman

A number of commercially available microcircuit resistors (Signetics PF860T and PF861T; Fairchild μER-1 and KRAA) and some custom-made Autonetics resistors were irradiated using a Field Emission Corporation 600-kilovolt flash X-ray machine. The beam was filtered by 64 mils of copper; 1.02 rads were deposited at a rate of 0.8×10^7 rad/sec for 0.12 microseconds during each irradiation. The dosimetry was performed by measuring the high-energy portion of the radiation spectrum using dental film and absorption techniques to filter out low-energy X rays. The film was calibrated using a 100-millicurie Cs^{137} source. The absorbed dose was then calculated assuming a Bouchard-type spectrum.

The noncommercial resistors tested were made by Autonetics in their Geographically Centralized Microelectronic Laboratory (GCML). Included in the tests were a diffused-silicon integrated-circuit resistor, polycrystalline-substrate semiconductor integrated-circuit resistors, nichrome thin-film resistors on a glass substrate, and a noble-metal/ceramic printed matrix on a ceramic substrate (CPC).

The photocurrent through the resistors was measured as a function of the bias voltage across the resistors. (The test circuit is shown in figure 2.) The results were interpreted to be in agreement with those expected from the transistor action because of the substrates present. The transistor-like nature of the parasitics due to construction of the integrated-circuit resistor is shown in figures 3 and 4, view (A). Figure 4, view (B), shows the equivalent circuit under irradiation exclusive of the transistor photocurrents. Typical results appear in figures 5 and 6.

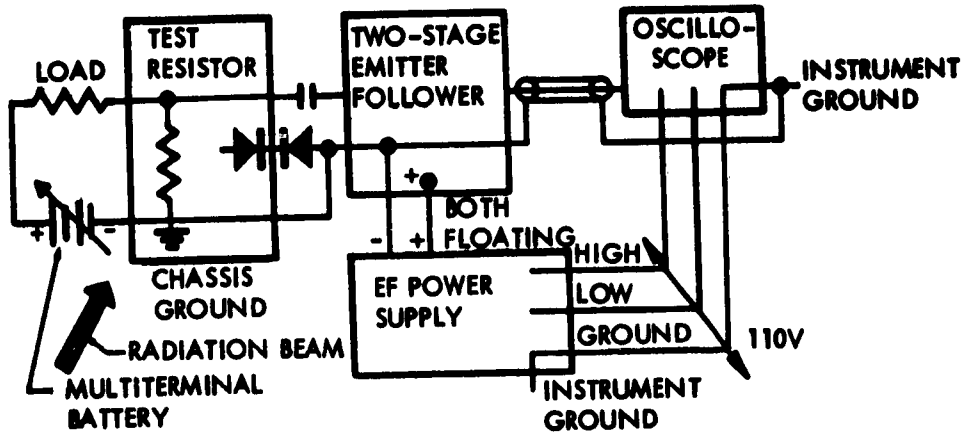

Figure 2. Test circuit.

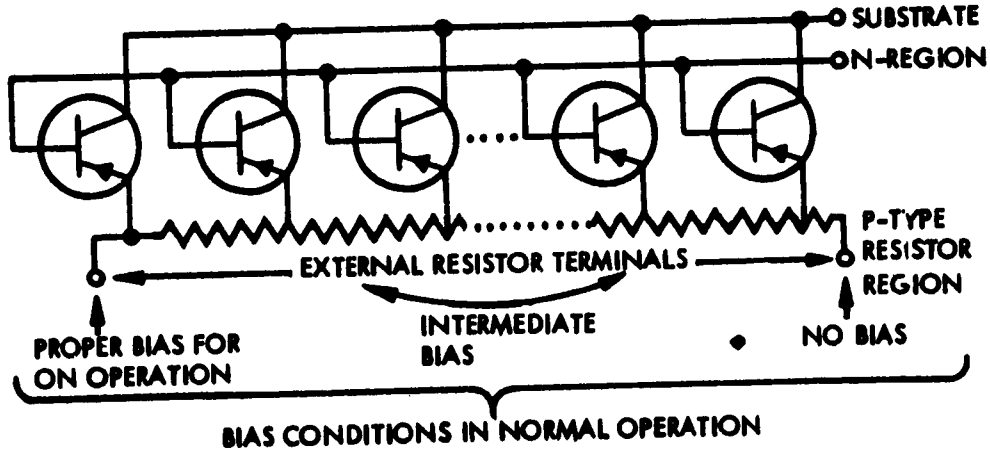

Figure 3. Generalized equivalent circuit of a diffused resistor.

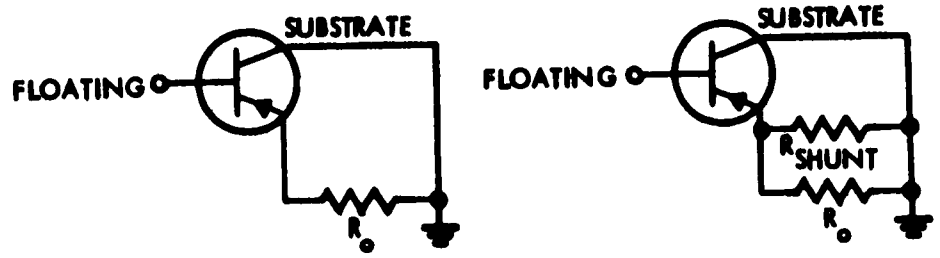

(A) NO IRRADIATION

(B) UNDER IRRADIATION A PHOTO-CURRENT WILL FLOW IN THE FORWARD DIRECTION

Figure 4. Simplified equivalent circuit (substrate grounded).

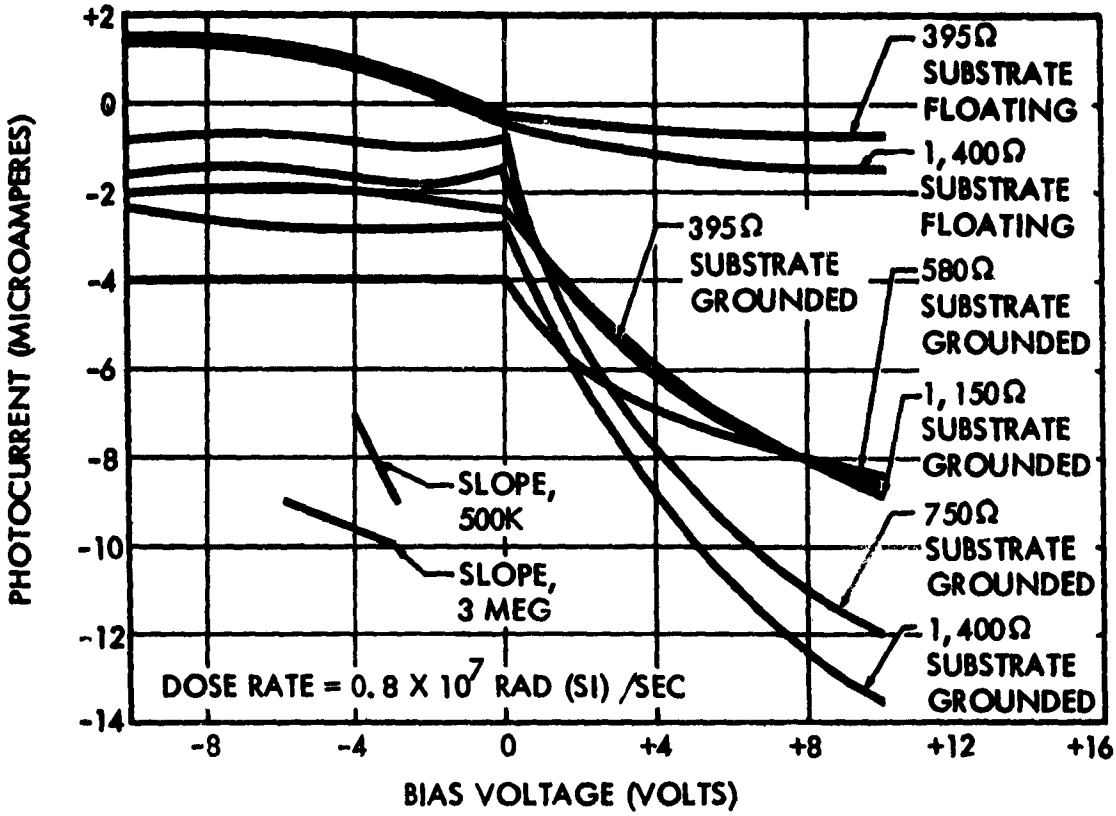

Figure 5. Photocurrent versus bias voltage for Fairchild resistors μER-1.

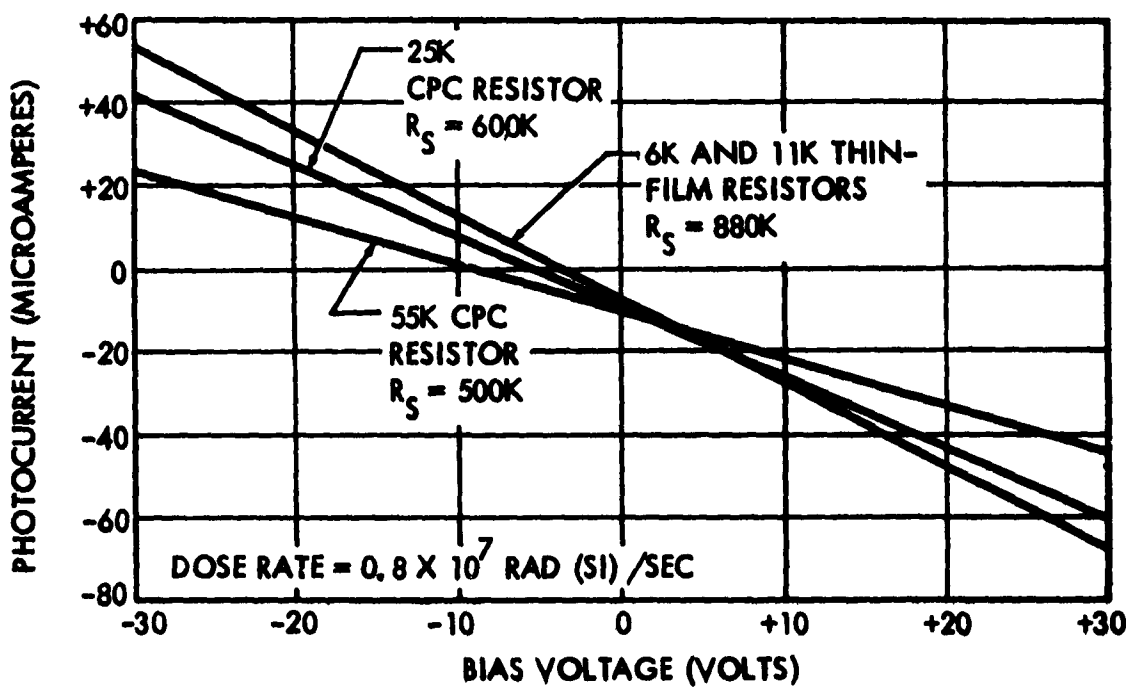

Figure 6. Peak photocurrent versus bias voltage for thin-film and CPC resistors.

ABSTRACT 3: AUTONETICS

Final Test Report on N17 Parts TRIGA Test Program, March 1964

A number of integrated circuits were irradiated to a total dose of approximately 3.5×10^{12} nvt ($E_n > 10$ kev) at the General Atomic advanced TRIGA prototype reactor. Circuits studied were TI mode 1 general purpose amplifier (GPA), TI mode 2 GPA, TI mode 3 GPA, standard chopper, TI driver switch, and RCA power switch. The results for the GPA circuits are summarized as follows:

GPA Circuit	Gain	Z_{in}	Differential Input Voltage Offset	Common Mode Output Voltage Offset
Mode 1	I: 20%	D: 50%	D	D
Mode 2	D: 40%	D: 40%	C	D
Mode 3	---	D: 40%	C	D
Mode 4	D: 15%	D: 35%	C	D

C = Constant D = Decreased I = Increased

The chopper showed no significant effects to a total dose of 3.4×10^{12} nvt. Similarly the driver switch showed no significant effects to 3×10^{12} nvt. The power switch I_{CEO} showed no effects up to a total dose of approximately 3×10^{12} nvt. V_{SAT} increased approximately 10 percent and beta decreased approximately 50 percent at I_C = 50 milliamperes and about 35 to 40 percent at I_C = 2.0 amperes for an integrated neutron flux of 3×10^{12} nvt.

Loading for the circuits was resistive and all tests were dynamic. Temperatures during the experiment were not specified.

ABSTRACT 4: BATTELLE MEMORIAL INSTITUTE

"Effects of Nuclear Radiation in Microcircuits," paper presented at the National Electronics Conference, Chicago, Illinois, October 19, 1964

Authors: R. B. Sorkin and D. J. Hamman

This report reviews the available data on the effects of nuclear radiation on silicon microcircuits. The scope is confined to permanent effects, as these effects are also more amenable to a component-by-component discussion. Displacement effects introduced by high-energy particles (electrons, protons, neutrons, and alpha particles) and to a lesser extent electromagnetic radiation (gamma and X rays) are discussed.

ABSTRACT 5: BELL TELEPHONE LABORATORIES, INC.

"Surface Effects of Radiation on Transistors," IEEE Transactions on Nuclear Science, Volume NS-10, No. 5, 35, November 1963

Author: R. R. Blair

The transistors tested included two integrated circuit transistors: Fairchild Type F and Texas Instruments SN310. The collector-base reverse current, I_{CBO}, and the current gain were measured as a function of absorbed dose from a Co^{60} source. The dosimetry was calculated from the irradiation time and a mapping of the environment.

Most of the effects can be qualitatively explained through the use of a simple model of the process: radiation ionizes the encapsulating gas, and the resulting ions and electrons are directed to transistor surfaces by electric fields existing at the junction surfaces and between the transistor and its can. Inversion layers are produced at the surface that grossly change certain transistor parameters. The great variability among devices of the same type suggests that the gases interact with the surface by imparting charge-to-surface contaminants. Results indicate that inversion layers on both collector and base are affecting I_{CBO}, while, as would be expected, gain is altered principally by an inversion layer on the base.

The results varied between device types; typical behaviors are shown in figure 7. Changes in the breakdown characteristic occurred at 1.3×10^8 rads. A similar change had been noted in similar transistors when they were exposed to 1.7×10^{15} fast neutrons/cm^2 at the Pennsylvania State University reactor, which has a mixed neutron-gamma environment.

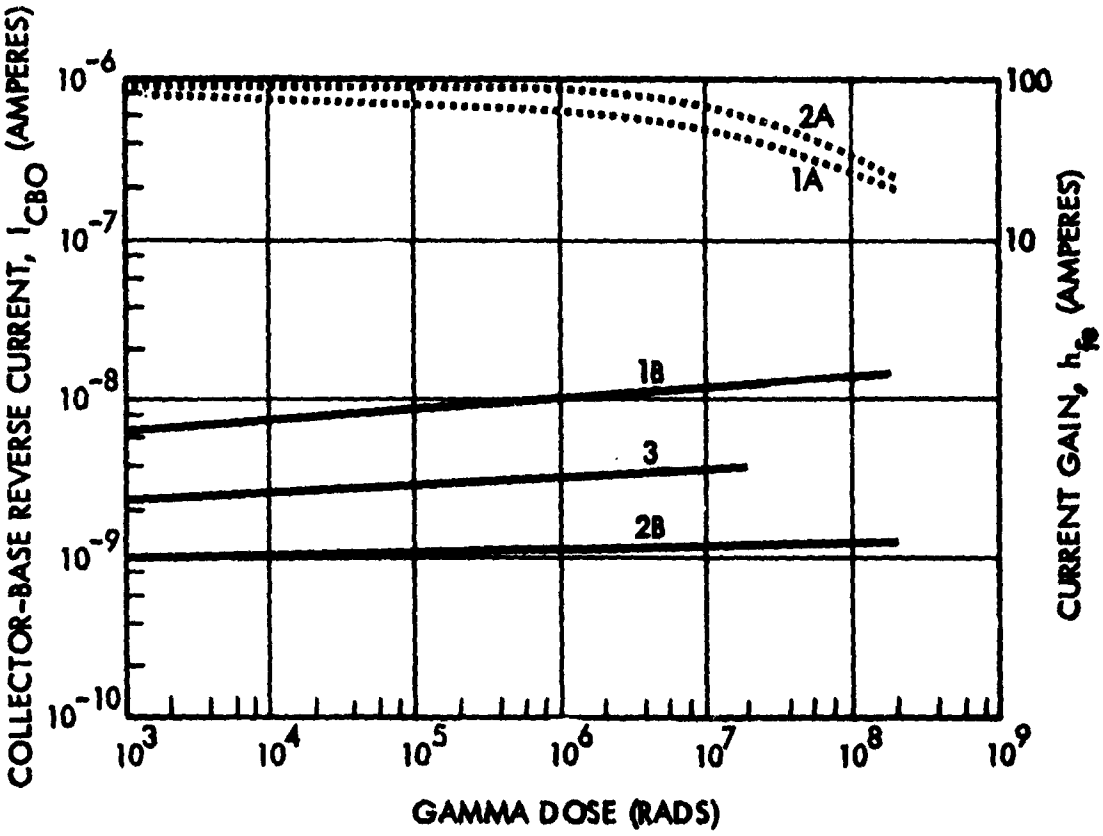

NOTES: 1. 1A, 1B INTEGRATED TYPE 1;
2A, 2B INTEGRATED TYPE 2;
3, TYPICAL OF TWO PLANAR TYPES.

2. $V_{CB} = 4.5V$

3. DOSE RATE = 6.5×10^5 RADS/HR

4. —— I_{CBO}
..... h_{fe}

Figure 7. Radiation response of I_{CBO} and h_{fe} of integrated transistors of types 1 and 2.

ABSTRACT 6: THE BENDIX CORPORATION

X-Ray Irradiation of Microcircuit "NOR" Gate Active Elements, May 14, 1964

Authors: D. Nelson and L. Laniewski

Three types of RTL NOR gates (Amelco G11-001, General Microelectronics D412, and Raytheon RC103) were irradiated using a Siefert Isovolt 150-kilovolt constant-potential X-ray machine.

The circuits were passive through the initial 1.8×10^7 R of exposure, then 3 volts were applied to the circuits. Three units were operated in a saturated mode while three units were operated cut off until a total exposure of 3.7×10^7 R had accumulated. The exposure rate was 4×10^5 R/hr. The dosimetry was by means of film and thermoluminescent dosimeters. During the irradiation, h_{fe} (at I_C = 2.5 milliamperes) and V_{SAT} (I_C = 1, I_B = 0.1 milliampere) were monitored on the circuit transistors and compared with unexposed samples. In addition, the junction breakdown voltage and leakage currents were measured before and after the irradiation. The significant changes that occur in the breakdown voltage as a result of irradiation are shown in table VI. Variations in gain during irradiation were similar for each circuit type. A typical data sample is shown in figure 8.

Table VI. Collector-to-Base Breakdown Voltage for X-ray Irradiated Devices

Unit No.	Manufacturer	BV_{CBO} at I_C = 5 μa		
		Before X ray	After X ray	After 120°C Bake
1	Amelco	13.5v	16.6v	Failure
2	Amelco	14.2v	19.6v	*14.4v
5	General Microelectronics	12.2v	16.7v	15.6v
6	General Microelectronics	9.5v	19.9v	*17.4v
9	Raytheon	26.5v	39.5v	36.5v
10	Raytheon	26.0v	34.5v	*28.0v

*These units were forward biased during the bake cycle.

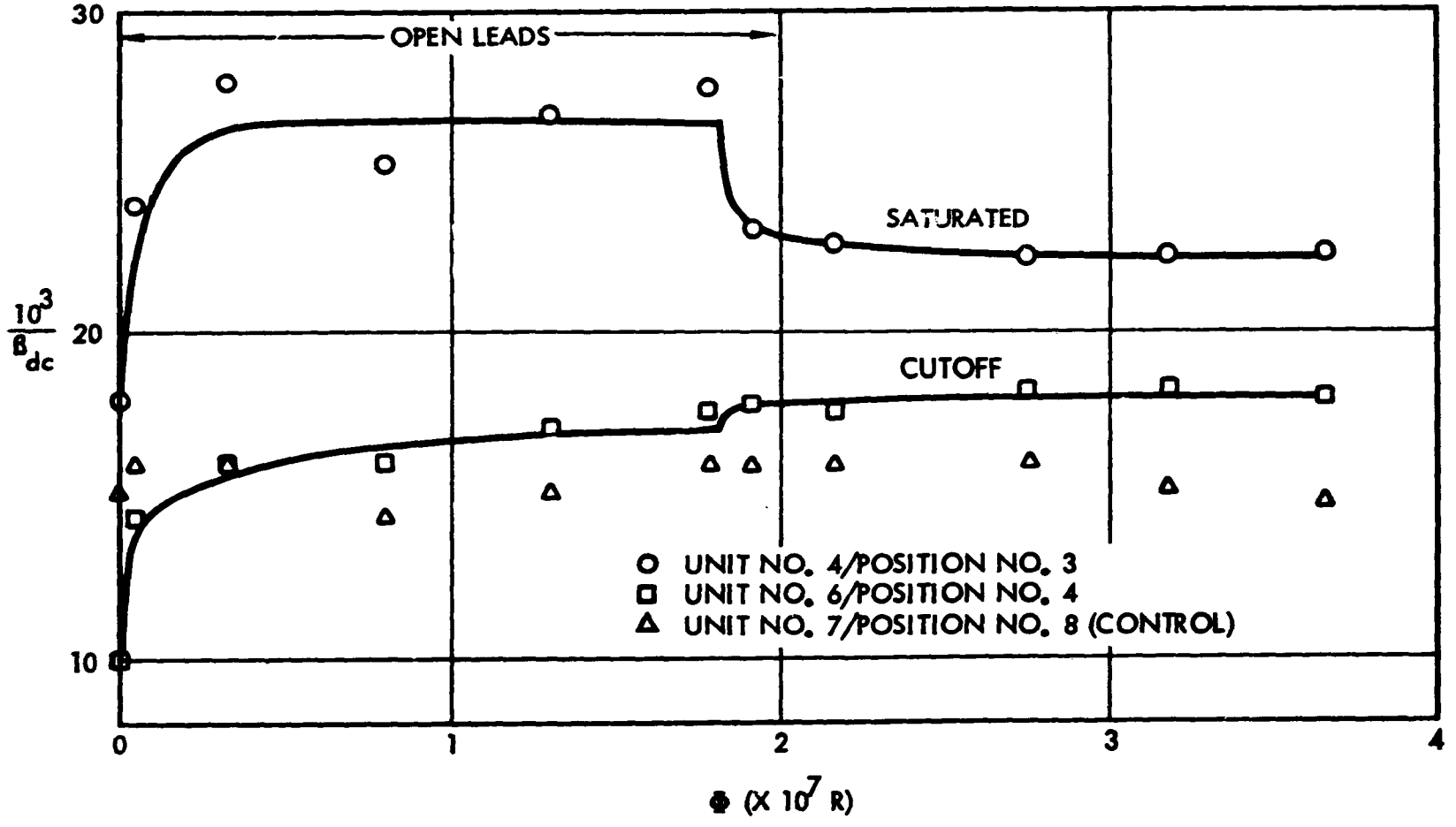

Figure 8. General Microelectronics Type D412 NOR gate.

ABSTRACT 7: THE BOEING COMPANY

"Transient Radiation Effects in Semiconductor Integrated Circuits," paper presented at IEEE National Winter Convention on Military Electronics, Los Angeles, California, February 1964

Authors: R. S. Caldwell and D. Nyberg

The transient responses of individual transistors and capacitors used in the Texas Instruments Series 51 circuits were measured using the Boeing 480-kvp flash X-ray machine. Dosimetry was based on measuring the exposure with air-equivalent dosimeters and converting to absorbed dose in the sample using large conversion factors determined both theoretically and experimentally. The radiation pulse widths were 0.2 microsecond.

The components tested were isolated electrically from the rest of the integrated circuit by scribing the evaporated aluminum leads at certain places and attaching additional ball-bonded gold wire leads where necessary. Electrical characteristics of the devices were checked after this isolation process to insure that no damage had occurred to the components.

A large delayed secondary photocurrent pulse (i_{sp}) was observed in the transistors (as shown in figure 9) when the p-region substrate was left floating; however, this current was drastically reduced both in magnitude and in time duration when the substrate was connected as in the normal circuit (reverse biased). These results and other measurements on these transistors of the primary photocurrents flowing at the various junctions indicated that the presence of the reverse-biased substrate junction was actually reducing the transient signal that the transistor would normally exhibit by draining off free carriers that would otherwise contribute to the primary photocurrent of the device. Such competition for the available carriers would occur only if the substrate-collector junction were located closer than a diffusion length to the base-collector junction. It was suggested that this construction technique might be useful in reducing transient currents in "normal" transistors.

Since capacitors in these circuits consist simply of reverse-biased p-n junctions connected in parallel, it was considered probable that the transient current pulse should be similar to junction photocurrents. The prompt portions of these currents were expected to be dependent on some fractional power of the applied voltage in the same way that capacitance varies with voltage; therefore, the voltage dependences of the capacitor photocurrents were measured as was the capacitance. As shown in figure 10, each quantity exhibited the same one-third power dependence as was expected, thus verifying the predictability of transient responses in microcircuit capacitors of this type and general size (100 to 200 picofarads).

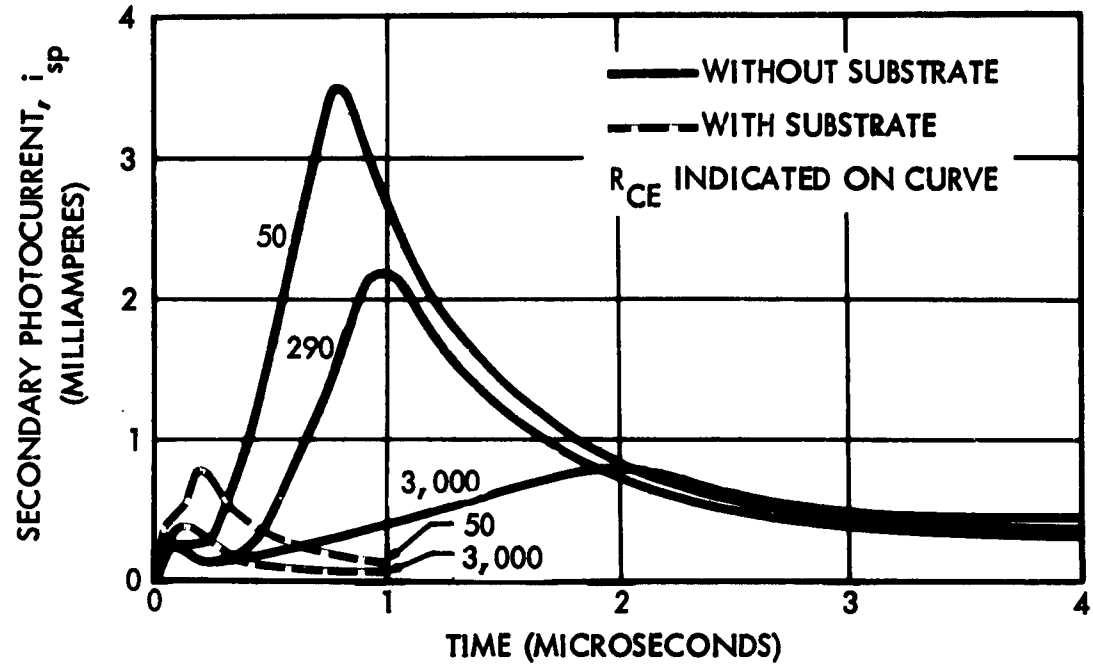

Figure 9. Observed secondary photocurrents in SN511 transistor during 480-kvp pulse at 10^7 rad/sec for 0.2 μsec.

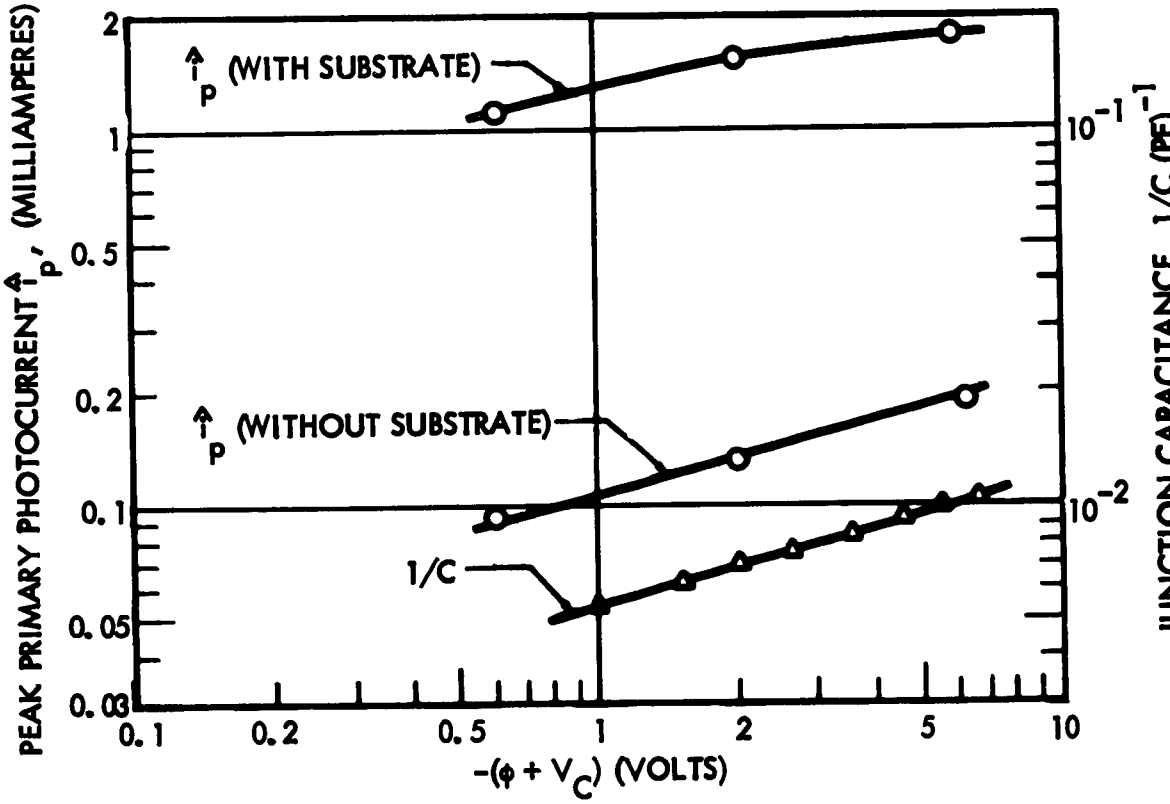

Figure 10. Observed voltage dependences of capacitance and primary photocurrents in SN511 capacitor during 480-kvp X-ray pulse at 10^7 rad/sec for 0.2 μsec.

ABSTRACT 8: THE BOEING COMPANY

Seminar and Microcircuit Study, BSD-TR-64-171, September 1964

Authors: W. C. Bowman, R. S. Caldwell, R. H. Dickhaut, et al.

This report includes (1) a survey of circuit responses to ionizing pulses of radiation for 39 microcircuits of the monolithic silicon type, (2) a study of neutron degradation for 6 of these circuits, and (3) predictions of the transient response of 6 circuits to ionizing radiation.

In the survey the circuit response was measured as a function of dose rate from 10^7 rad/sec to 4×10^9 rad/sec for both minimum and maximum fanout conditions and, for some circuits, both output logic states. The radiation source used was a 0.2-microsecond pulse of 10-Mev electrons from the Boeing linear accelerator. The primary photocurrent from a 2N2243 transistor was used as a secondary-standard dosimetry monitor and was calibrated against glass rods. The roentgen-to-rads (Si) ratio was calculated to be 0.91 for 10-Mev electrons. The outputs of the logic circuits were loaded with resistor-diode circuits that simulated the gate units of each logic family. The inputs were loaded resistively to simulate a gate unit at maximum fanout. The amplifiers were resistively loaded. A typical set of data presented for each of the 39 circuits is shown in figure 11.

The failure point for each circuit was determined by the amplitude of the response necessary to switch the gate loading the output and by the radiation level required to give that response. The loading gate was considered to have switched when the midpoint of the transition region of the gate transfer characteristics was reached. The transient failure criterion for the amplifiers was defined at the point where the output signal was sufficient to drive the loading gate circuit from ground to the switching threshold.

The results are summarized in table VII. Failure levels have been given either for dose rates or for total doses. When the output reaches an equilibrium level below saturation and during the radiation pulse, the devices are listed as dose

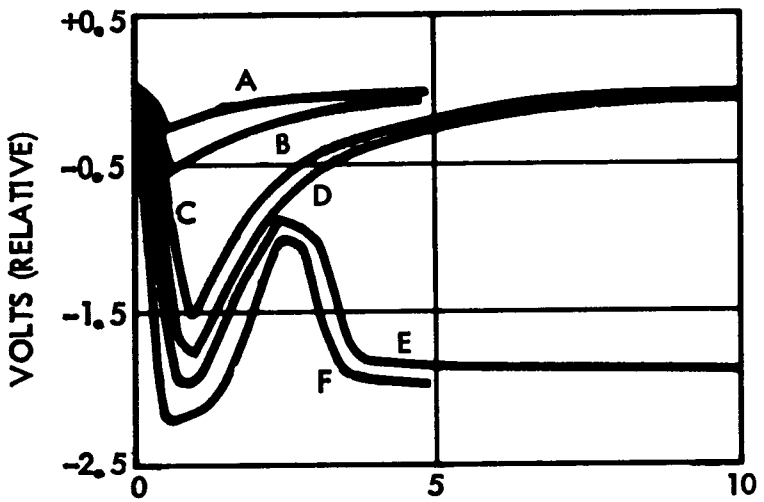

RESPONSE FOR FANOUT 1

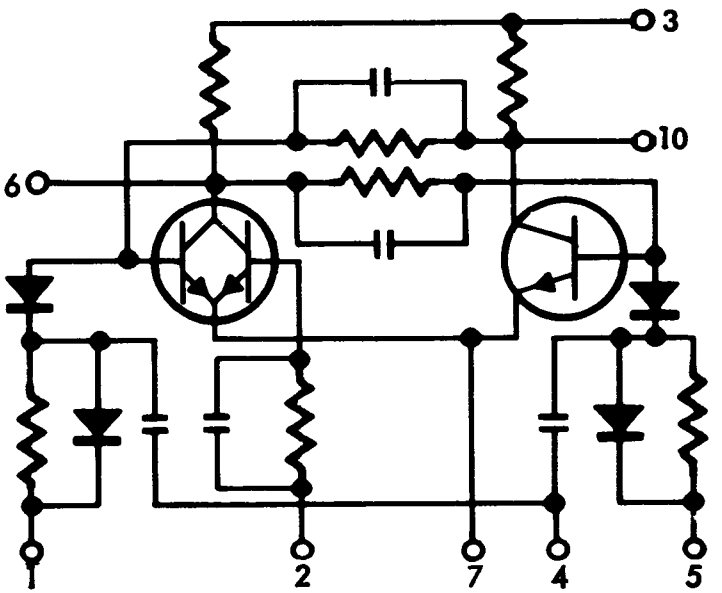

SCHEMATIC

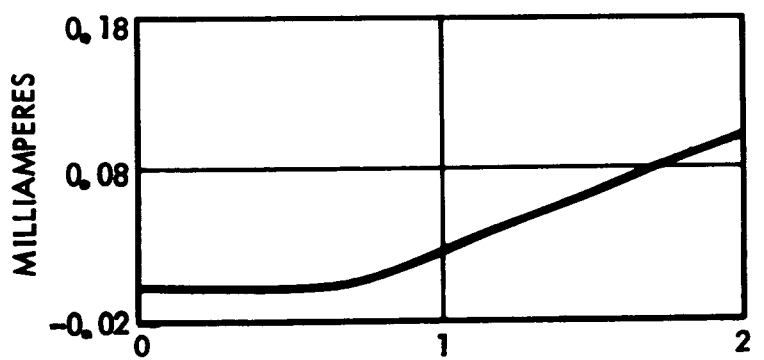

LOAD CHARACTERISTICS FOR FANOUT 1

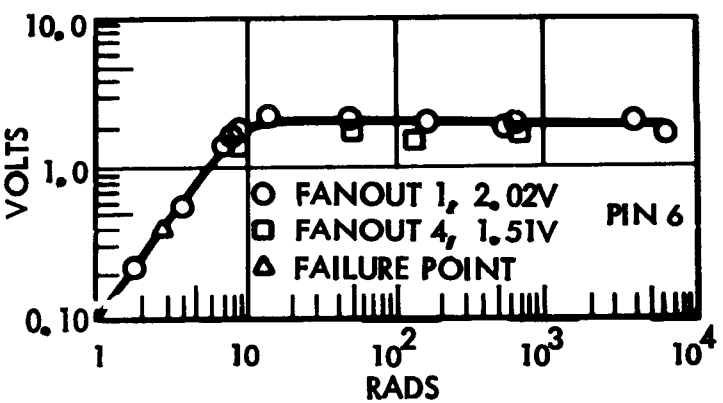

MAXIMUM DEFLECTION VERSUS DOSE

Figure 11. SN510.

Table VII. Microcircuit Survey

Component	Manufacturer	Designation	Failure Dose/Dose Rate		Extended Duration at 10^3 rads (μsec)	dI_{cc} at 600 rads (ma)
			Min. Fanout	Max. Fanout		
Gate	Fairchild	μL903	3×10^8 rad/sec	1.6×10^8 rad/sec (0.08 μsec)	0.4, D	---
		MWμL910	2.5×10^8 rad/sec	1.6×10^8 rad/sec (0.1 μsec)	2.4, D	<25
	General Microelectronics	G	1.6×10^8 rad/sec	1.6×10^8 rad/sec (0.1 μsec)	0.6, D	---
		D_2	4.5×10^8 rad/sec	2.5×10^8 rad/sec (0.1 μsec)	1, D	<28
	Honeywell	MHM3001	40 rads*	34 rads*	5, D	88
		MHM3101	36 rads	23 rads	1.3, S	71
	Melpar	MM1001	14 rads*	15 rads*	5, B	95
	Motorola	MC306G	1.1×10^8 rad/sec	1.1×10^8 rad/sec (0.06 μsec)	12, S	520
	Pacific Semiconductor	PCG102	3×10^8 rad/sec	5×10^8 rad/sec (0.12 μsec)	1, D	35
	Raytheon	RC103	9×10^7 rad/sec	9×10^7 rad/sec (0.06 μsec)	0.7, D	<49

* The circuit output is in a "0" logic state. The output of the other devices is in a "1" logic state.

Table VII. Microcircuit Survey (Continued)

Component	Manufacturer	Designation	Failure Dose/Dose Rate		Extended Duration at 10^3 rads (μsec)	dI_{cc} at 600 rads (ma)
			Min. Fanout	Max. Fanout		
Gate	Signetics	SE102	40 rads*	40 rads*	5, D	<25
		SE110	50 rads	50 rads	1, D	29
	Siliconix	A01A	22 rads	30 rads	2, D	110
	Sylvania	SNG-3	4×10^8 rad/sec	5.5×10^8 rad/sec ($0_{\text{p}}12$ μsec)	0.7, D	21
		SNG-7	9×10^8 rad/sec	10^9 rad/sec (0.06 μsec)	0.5, D	---
	Texas Instruments	SN514	6.5 rads	5 rads	10, S	300
	Transitron	3-input gate	3.2×10^8 rad/sec	4.2×10^8 rad/sec (0.1 μsec)	0.7, D	<63
	Westinghouse	WM201	15 rads	16 rads	3, D	140
Flip-Flop	Fairchild	μL902	2.3×10^8 rad/sec	2.3×10^8 rad/sec	0.4, D	<35
	General Microelectronics	R	2×10^8 rad/sec	1.3×10^8 rad/sec	1, D	<35
	Honeywell	MHM3201	60 rads	50 rads	0.43, D	75

* The circuit output is in a "0" logic state. The output of the other devices is in a "1" logic state.

Table VII. Microcircuit Survey (Continued)

Component	Manufacturer	Designation	Failure Dose/Dose Rate		Extended Duration at 10^3 rads (μsec)	dI_{cc} at 600 rads (ma)
			Min. Fanout	Max. Fanout		
Flip-Flop	Motorola	MC302G	3×10^7 rad/sec	4.2×10^7 rad/sec	3.5, S	440
	Pacific Semiconductor	PCF101	6×10^8 rad/sec	5×10^8 rad/sec	0.5, D	35
	Signetics	SE124	300 rads	40 rads*	10, D	155
	Texas Instruments	SN510	3.6 rads	3 rads	7, S	250
	Westinghouse	WM202	8 rads	4 rads	0.6, S	175
Amplifier	Fairchild	μC101	400 rads (50K)	400 rads (10K)	6.5, D	118
	Motorola	MC1110	10^9 rads/sec (3K)	4×10^9 rad/sec (1K)	3, B	---
	Pacific Semiconductor	PCD011	16 rads (10Ω)		500, D	---
	Texas Instruments	SN522	4 rads (gain 2)	4 rads (gain 10)	200, D	200
Schmitt Trigger	Pacific Semiconductor	PCS101	4×10^8 rad/sec	4×10^8 rad/sec	0.7, D	34

* The circuit output is in a "0" logic state. The output of the other devices is in a "1" logic state.

Table VII. Microcircuit Survey (Continued)

Component	Manufacturer	Designation	Failure Dose/Dose Rate		Extended Duration at 10^3 rads (μsec)	dI_{cc} at 600 rads (ma)
			Min. Fanout	Max. Fanout		
Half Adder	Fairchild	μL904	3×10^8 rad/sec	4×10^8 rad/sec	0.5, B	25
	General Microelectronics	A	7×10^8 rad/sec	4×10^8 rad/sec	0.6 B	---
	Motorola	MC303G	2.5×10^7 rad/sec	3.3×10^7 rad/sec	12, S	250
Buffer	Fairchild	μL900	3.6×10^8 rad/sec	1.2×10^8 rad/sec	0.55, D	---
	General Microelectronics	B	5×10^8 rad/sec	2×10^8 rad/sec	1.5, B	---
Multivibrator	Signetics	SE160	0.94 rads	0.94 rads	---	75
Half Shift Reg.	Fairchild	μL906	1.9×10^8 rad/sec	2.2×10^8 rad/sec	0.4, B	59
Bias Driver	Motorola	MC304G	35 rads	35 rads	5, S	230

* The circuit output is in a "0" logic state. The output of the other devices is in a "1" logic state.

B denotes that storage and decay time are equivalent.

S denotes that storage time is predominant.

D denotes that decay time is predominant.

rate dependent. The time to reach equilibrium is given in parentheses after the maximum fanout failure dose rate for the gates. When no equilibrium level is reached during the 0.2-microsecond radiation pulse (below saturation), the devices are listed as dose dependent. The extended duration measurement refers to the time required for the circuit to reach a stable state after the irradiation has ended. The shape of the pulse during extended duration is inferred as is indicated by a letter following the quoted time at 10^3 rads. These letter designations are defined at the end of the table.

Six circuits were studied for neutron degradation of their logic levels and switching times. Generally, power was applied during irradiation, but for two devices both powered and unpowered data were obtained. The circuits studied and the results obtained are listed in table VIII. Typical graphs of the data presented for each circuit are shown in figures 12 and 13.

The radiation source used was a photoneutron reaction in a uranium target at the Boeing linear accelerator using 25-Mev electrons. The fluence was determined by activation of sulfur foils and relating this to a previous map of neutron flux using fission and activation foils. Neutron fluence is related to the plutonium threshold of 10 kev. The circuits were loaded in the same fashion as for the transient tests. Failure occurred when the low logic level at the output degraded to the point where it no longer satisfied the voltage requirement for that logic state. Failure was due to transistor gain degradation.

Predictions of the transient responses were made using a charge control model for the transistor by combining the Beaufoy and Sparkes model and the Ebers and Moll model. The transistor action of the base-collector-substrate regions was included in the circuit schematic, which resulted in a more complex circuit diagram than is normally published by the manufacturer. (An example of such a circuit is shown in figure 14.) The primary photocurrents were measured at 10^8 rad/sec on the Boeing 480-kv flash X-ray machine and extrapolated to higher rates for comparison with the linear-accelerator data from the survey. The resulting predictions, although of varying degrees of success, indicate that the mechanisms of failure are

Table VIII. Neutron-Irradiated Microcircuits

Manufacturer	Designation	Type	Nominal Supply (volts)	Supply Status	Fan-Out	Failure Fluence (n/cm^2)
NOTE: Numbers in parentheses indicate particular circuit.						
Raytheon	RC103 (1)	Gate	+3	Powered	5	1.2×10^{15}
	RC103 (2)	Gate	+3	Powered	5	1.6×10^{15}
Honeywell	MHM3001 (1)	Gate	+3	Powered	5	1×10^{15}
Fairchild	μL903 (2)	Gate	+3	Powered	5	1.6×10^{15}
	μL903 (3)	Gate	+3	Powered	5	1.4×10^{15}
Signetics	SE102 (1)	Gate	+4, -2	Powered	10	7.5×10^{14}
	SE102 (2)	Gate	+4, -2	Powered	10	7.5×10^{14}
Motorola	MC304G (5)	Bias Driver	-5.4	Unpowered	25	$>1.5 \times 10^{15}$
	MC304G (6)	Bias Driver	-5.4	Powered	25	1.3×10^{15}
	MC304G (7)	Bias Driver	-5.4	Powered	25	1.5×10^{15}
Texas	SN510 (1)	Flip-flop	+3	Unpowered	4	10^{14}
	SN510 (2)	Flip-flop	+3	Powered	4	1.5×10^{14}
	SN510 (3)	Flip-flop	+3	Powered	4	10^{14}

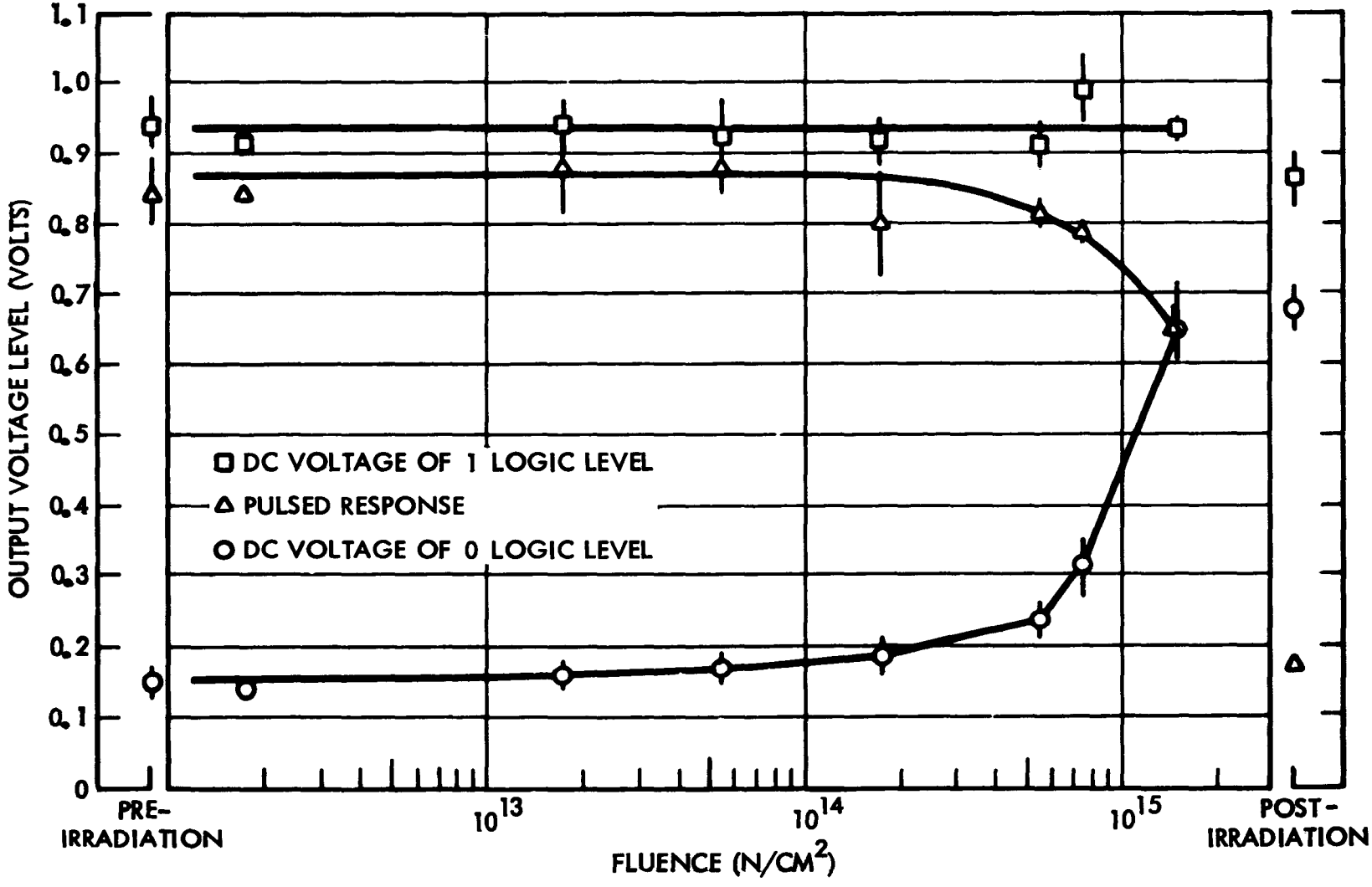

Figure 12. Neutron degradation of voltage levels at the output for μL903.

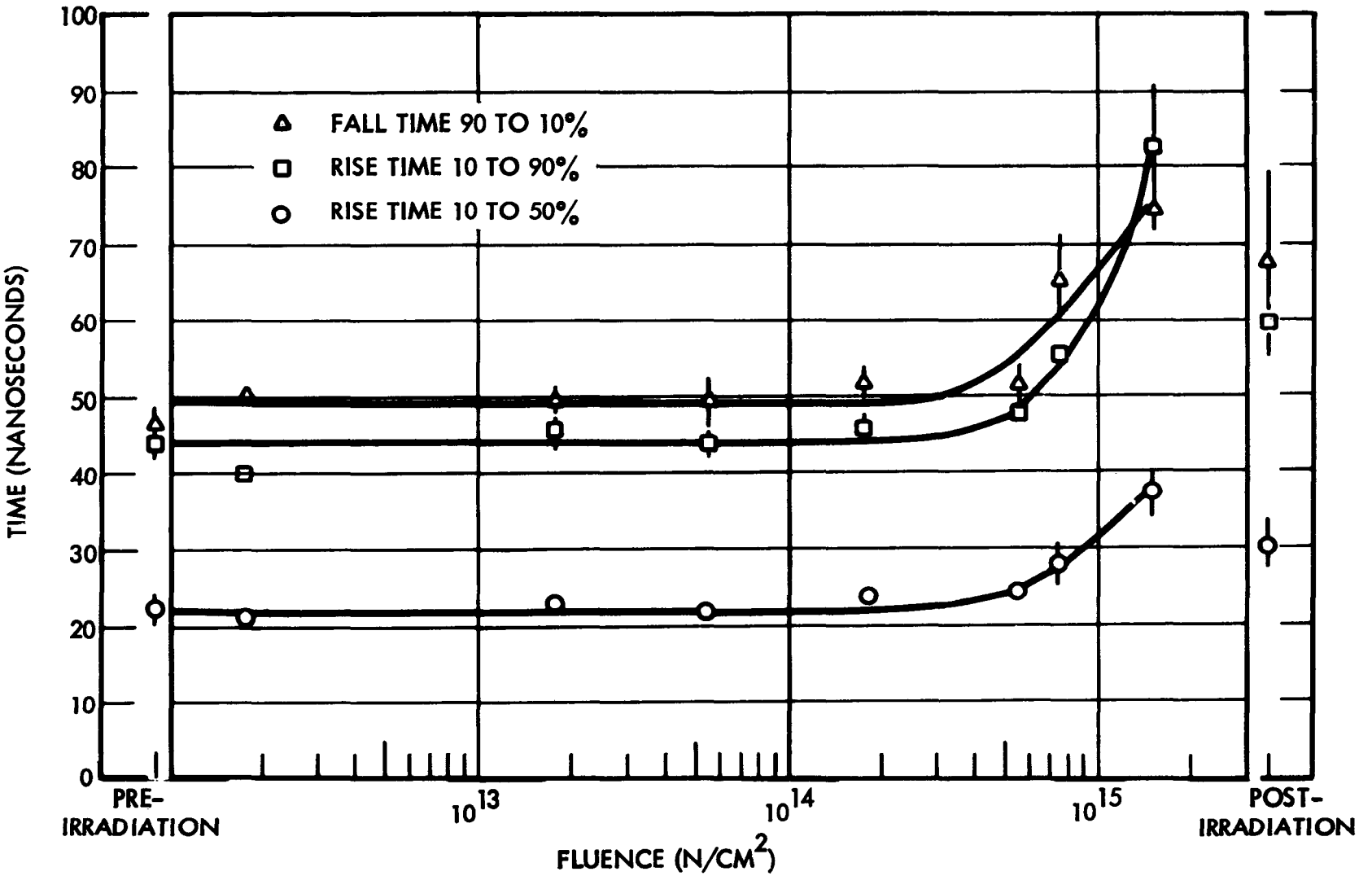

Figure 13. Neutron degradation of rise and fall times for μL903.

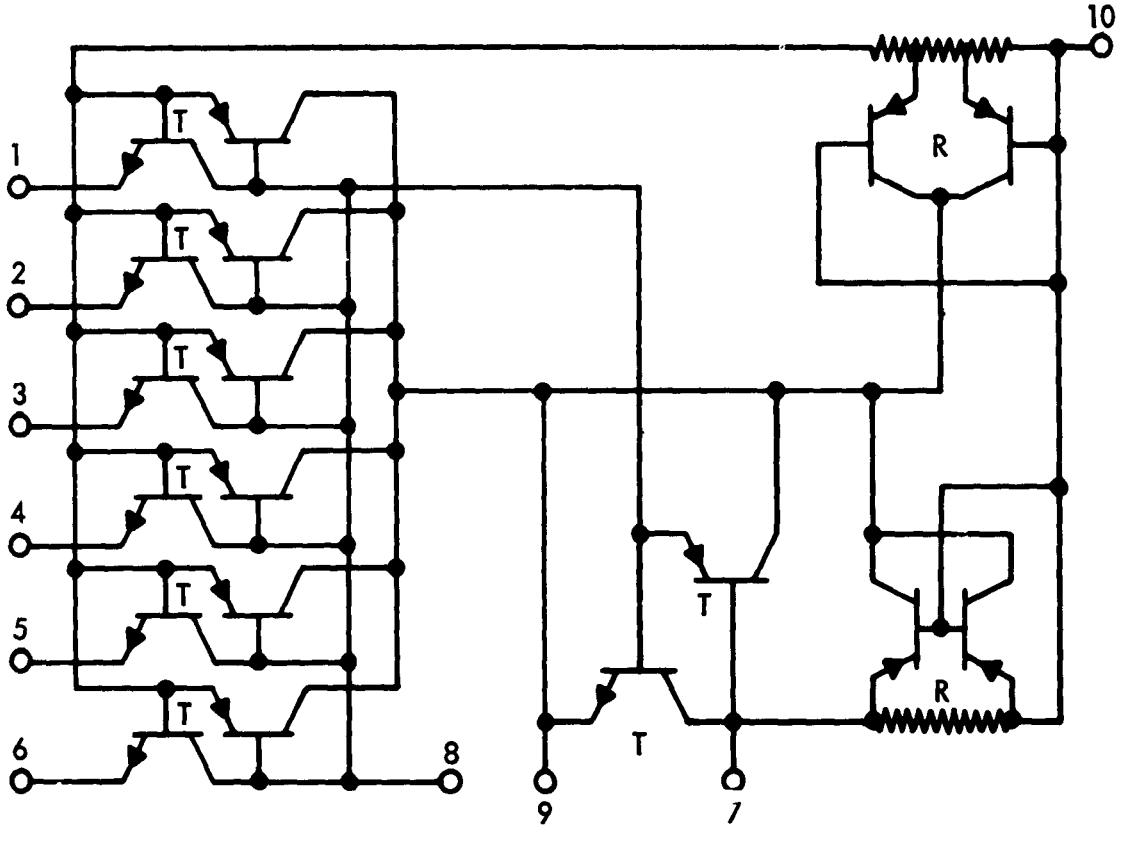

Figure 14. Topological equivalent circuit for MHM3001.

the shorting effect of the substrate current and the shunt currents developed across the resistors. A typical prediction result caused by a 0.2-microsecond radiation pulse is shown in figure 15.

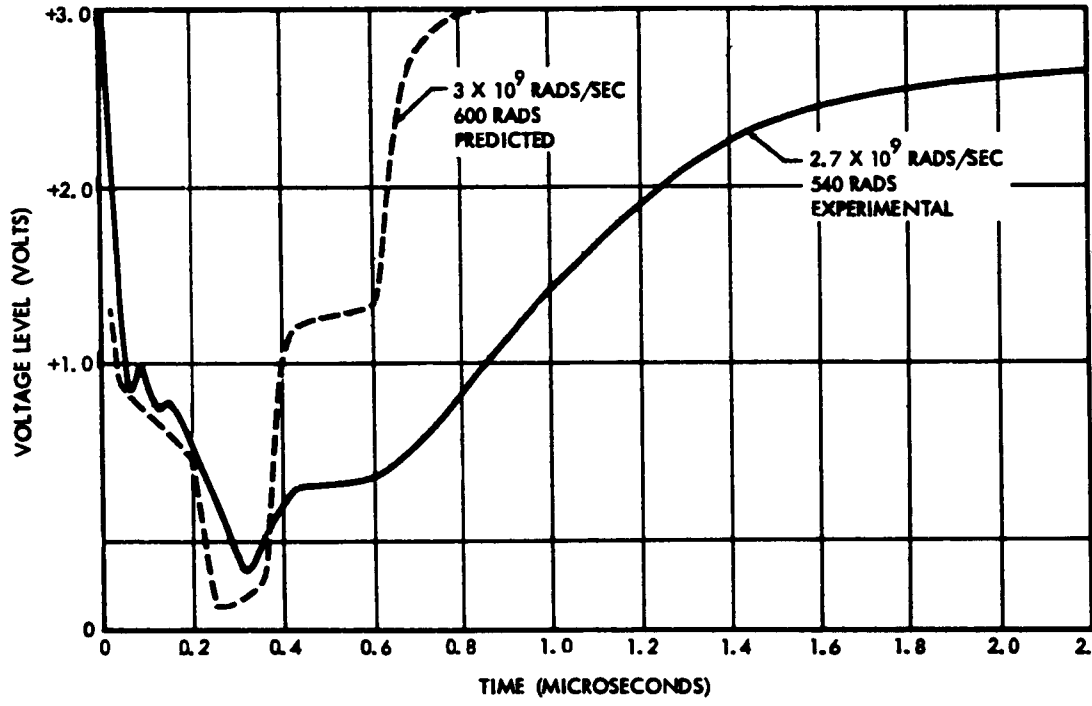

Figure 15. Measured and predicted response for MHM3001 with output logic level "1".

ABSTRACT 9: THE BOEING COMPANY

SABRE Radiation Effects Data Book, Boeing Document D2-90607, November 25, 1964

Authors: W. E. Butts, L. L. Hunter, and H. W. Wicklein

This document contains radiation effects and electrical test data on components and circuits used or proposed for the SABRE guidance system. It is a source book of data for determining system vulnerability and for supporting hardening of the system.

The transient radiation tests were performed at the Boeing linear accelerator using 10-Mev electrons. The dose rates used were between 2.5×10^5 and 3×10^{10} rad/sec with pulse lengths of 50 and 500 nanoseconds. The outputs of the circuits were loaded generally in the same manner as they are in the system. Most integrated circuits were tested with two initial static states, "on" and "off." Amplifiers were tested in a single state.

Neutron irradiation tests were made using photoneutrons from bombardment of a thick U^{238} target by 25-Mev electrons from the Boeing linear accelerator. The parameters measured depended on the type of circuit tested. For the logic elements, logic states were measured with a simulated load applied. The output levels of the amplifiers were monitored using a 1-millisecond input pulse. Proper loading was maintained for the amplifiers. All circuits were irradiated to a fluence of 1×10^{14} to 3×10^{14} n/cm^2. A number of significant parameters were measured after various neutron doses up to the maximum dose. All devices were irradiated statically. Table IX lists the 30 circuits tested.

An addendum to Boeing Document D2-90607 contains additional neutron data that have been obtained for the following circuits: SFF3A, SFF15, TNG3211, XC201, μL931, μa702, and a Norden special differential amplifier.

Table IX. Proposed SABRE System Components Tested

Microcircuits	Description	Manufacturer
7900309/C1063	Logic element	Signetics
7900309/WS268Q	Logic element	Westinghouse
7900310/C1050	Logic element	Signetics
7900310/WS269Q	Logic element	Westinghouse
7900311/C5051G	Logic element	Signetics
7900311/WS208Q	Logic element	Westinghouse
7900312/C1052	Logic element	Signetics
7900312/WS270Q	Logic element	Westinghouse
7900313/C1053G	Logic element	Signetics
7900313/WS271Q	Logic element	Westinghouse
7900314/C1054	Logic element	Signetics
7900314/WS272Q	Logic element	Westinghouse
7900315/WS130	Dual matching circuit	Westinghouse
7900316/WS131	D-A switch	Westinghouse
7900317/WS8149	Diverter driver	Westinghouse
7900319/C1055	Sense amplifier	Signetics
7900320/C1073	Sense amplifier gate	Signetics
7900322/SE160G	Monostable multivibrator	Signetics
7900324/WS133Q	DRO bit driver	Westinghouse
7900325/C1065G	Diverter gate	Signetics
7900326/WS135	Dual Darlington	Westinghouse
SE101G	Logic element	Signetics
SE105G	Logic element	Signetics
SE124G	Logic element	Signetics
CS701	Logic element	Signetics
SNG5A	Logic element	Sylvania
113K3	Dual emitter chopper	Sperry
FMC108	Schmitt trigger	Fairchild
FMC110	Darlington differential amplifier	Fairchild
FMC111	Buffer differential amplifier	Fairchild

ABSTRACT 10: THE BOEING COMPANY

Predicting Transient Radiation Effects on Electronic Circuits, Final Report on AFWL Contract AF 29(601)-6425, to be published about June 1965

Authors: W. C. Bowman, R. S. Caldwell, D. Duncan, et al.

Four microcircuits were tested intensively at the Boeing linear accelerator with 10-Mev electrons. Dosimetry was based on glass rods. Dose rates ranged from 8.3×10^7 to 6.8×10^9 rad/sec (0.2-microsecond pulse) on two thin-film hybrid microcircuits (IRC HD 903 gate and Varo 8201 amplifier). The dose rate for the two monolithic circuits (Motorola MC356G gate and Fairchild μL900 buffer) was 3×10^9 rad/sec. All circuits were loaded to a fanout of 1 by resistor-diode loads simulating the load of a subsequent circuit. Components were isolated and the responses measured for each component under a variety of conditions. Output responses were measured for each circuit. Computer predictions conducted for the output response for each of the circuits are presented.

ABSTRACT 11: BURROUGHS CORPORATION

"Effects of Nuclear Radiation on Integrated Circuits Performance," paper presented to the joint meeting of the Philadelphia sections of IEEE Groups on Reliability and Electron Devices, October 13, 1964

Authors: Francis T. Lynch and William F. Valitski

In the first group of experiments, the Fairchild μL914 was assumed to be typical of resistor-transistor logic (RTL) and was exposed to the steady-state neutron/gamma flux of the Pennsylvania State University (PSU) nuclear reactor facility. The second group of experiments was performed at the Sandia pulsed reactor facility (SPRF) and included the Motorola MC306, which was assumed to be typical of the emitter-coupled logic (ECL).

The dosimetry was performed using sulfur-activation techniques. At SPRF the neutron flux was related to the 10-kev plutonium threshold using the value of 7.2 for the plutonium-to-sulfur ratio; at PSU the sulfur level was related to a 100-kev threshold using a measured neutron spectrum. To obtain integrated flux numbers that would be the equivalent of the SPRF exposures, a correlation factor of 1.5 was used. This factor is the ratio of the lifetime damage constant at PSU to that constant at SPRF on two identical batches of silicon planar transistors.

During irradiation the circuits were unpowered. The logic level voltages were measured for groups of two or three circuits removed at various dose levels. A total of 15 μL914 and 21 MC306 circuits were exposed to various fluences up to 4.1×10^{14} n/cm^2 ($E_n > 10$ kev).

The results, which can be explained in terms of transistor gain degradation, are shown in figure 16. The more pronounced change in RTL is due to the stronger dependence of ß on collector-emitter voltage when the transistors are in saturation than when they are operating in their active region, as is true for ECL.

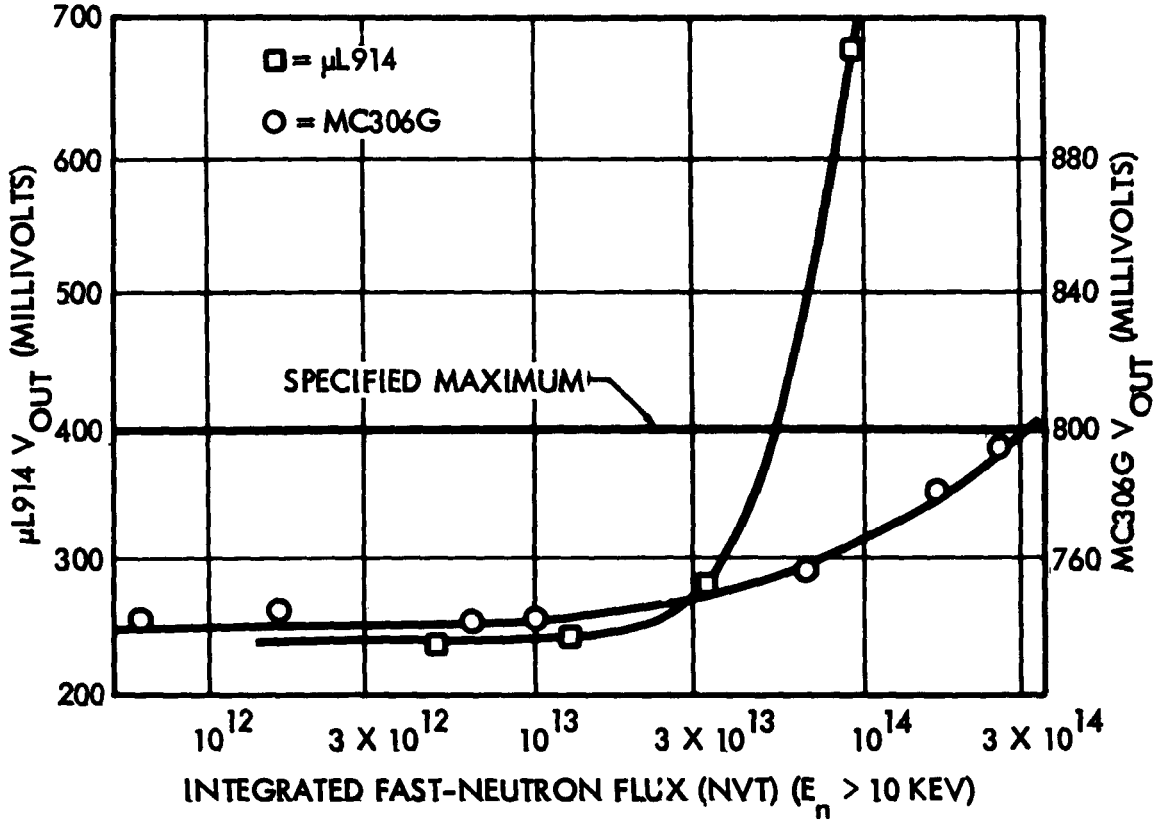

Figure 16. ECL and RTL output voltage versus neutron exposure.

ABSTRACT 12: BURROUGHS CORPORATION

Determination of Semi-Conductor Device Figure of Merit (appendix), Report No. 4, Signal Corps Contract DA-36-039-AML - 02366(E), Department of Army Project (OST) 74-01-004-36, Final Report, July 1, 1964

Authors. F. Barsam, A. Long, and F. Lynch

In addition to a restatement of the permanent damage data presented in "Effects of Nuclear Radiation on Integrated Circuits Performance," by F. Lynch and W. Valitski (Abstract 11), data are presented on the transient response of a μL914 to 20 bursts of the SPRF reactor. The neutron fluence was measured by sulfur activation and can be related to the spectrum above 10 kev by the previously determined plutonium-to-sulfur ratio, 7.5. The absorbed dose in rads (C) was calculated from the exposure dose measured using glass rods.

Figure 17 shows the test circuit used. The input and output currents and voltages were measured and are tabulated. No failures were observed. Table X contains the measured response of μL914 transient response at SPRF.

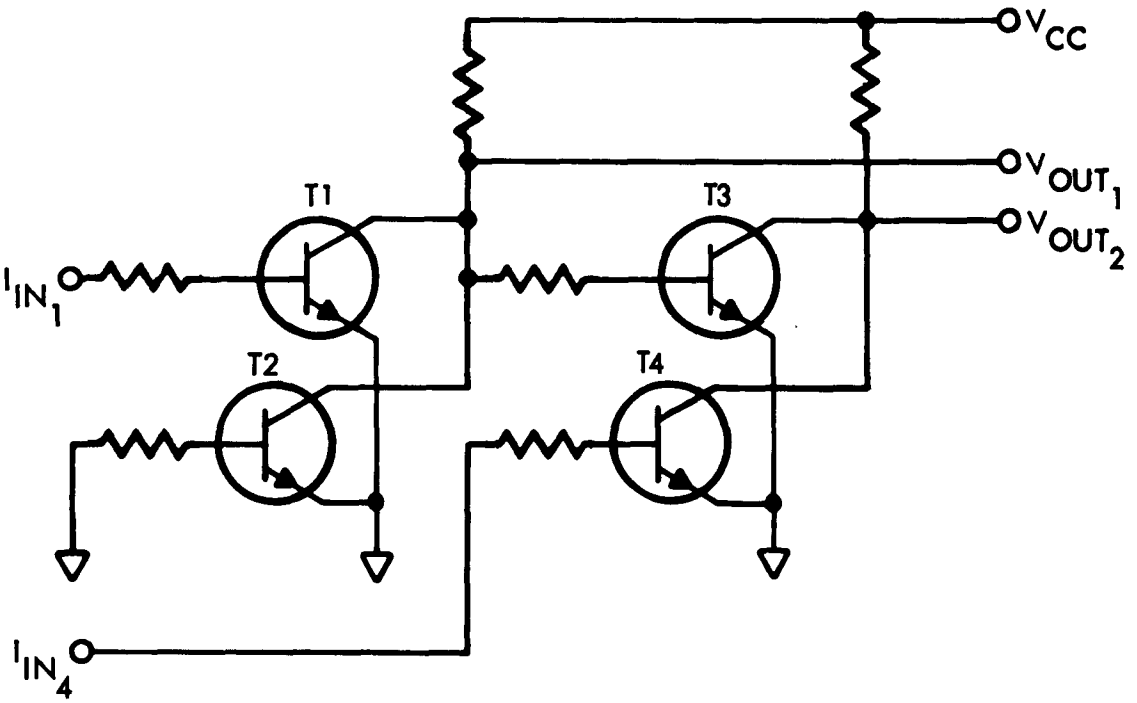

Figure 17. Test circuit of dual two-input RTL gate.

Table X. Transient Experiment Data

Input Volts		Transient		Transient		Exposure		Number (Unit-Shot)
T_1	T_2	ΔI_{IN_1} (μa)	ΔI_{IN_4} (μa)	ΔV_{OUT_1} (mv)	ΔV_{OUT_2} (mv)	Rads/Sec (Carbon)	Nvt E>3 Mev	
0.554	0.554	-8	-6	-21	+4	3(7)	4(11)	10-3154
		---	---	-10	+9	5(7)	1(12)	14A-3164
0.554	0.844	+28	+7	-35	+2	3(7)	1(12)	4-3148
		+40	-10	---	---	---	---	K0-3141
		+76	+65	-50	>+4	5(7)	1(12)	2-3146
		+36	+18	-37	+8	4(7)	1(12)	3-3147
		-10	+4	-10	+9	6(7)	1(12)	13A-3163
0.844	0.554	+40	-10	+20	<2	4(7)	1(12)	5-3149
		+36	-20	+15	<2	4(7)	1(12)	K9-3142
		-14	-10	+24	<1	3(7)	1(12)	K8-3143
		+64	+32	---	---	4(7)	1(12)	1-3145
		+22	-2	+15	-0.15	2(7)	4(11)	6-3151
		+31	---	>+15	-0.25	2(7)	6(11)	6-3155
		---	---	+8	-0.40	2(7)	5(11)	12A-3162
		-20	-1	+14	-0.90	6(7)	1(12)	15A-3166
0.844	0.844	-7	-3	+10	-14	2(7)	5(11)	9-3153
		-5	-1	1	1	2(7)	5(11)	7-3150
		-5	-4	---	---	2(7)	5(11)	8-3152
		-4	-4	+10	+20	2(7)	5(11)	9-3156
		-9	-7	+8	+8	2(7)	5(11)	11A-3161

ABSTRACT 13: DOUGLAS AIRCRAFT COMPANY

Development of Radiation Resistant Digital Circuits, Douglas Report SM-45766, October 22, 1963

Author: B. J. Donaldson

A number of Texas Instruments Series 51 microcircuits were exposed to the radiation environment of the UCLA training reactor facility. The dosimetry was computed from a spectrum mapping done by UCLA using foil activation techniques. The circuits were interconnected as shown in figure 18. Their output voltages and switching times were monitored using Nuvistor cathode followers to drive the 60 feet of coaxial cable required to reach the control room. The circuits failed between 1.8×10^{14} and 5×10^{14} n/cm^2 ($E_n > 0.4$ ev) as shown in figures 19 and 20. The neutron flux was 7×10^{10} n/cm^2-sec and the gamma dose rate was estimated to be 10^6 rad/hr. The flip-flops were first to fail. The epicadmium fluence is used rather than that above the plutonium threshold because the UCLA reactor spectrum is heavily weighted at the lower neutron energies.

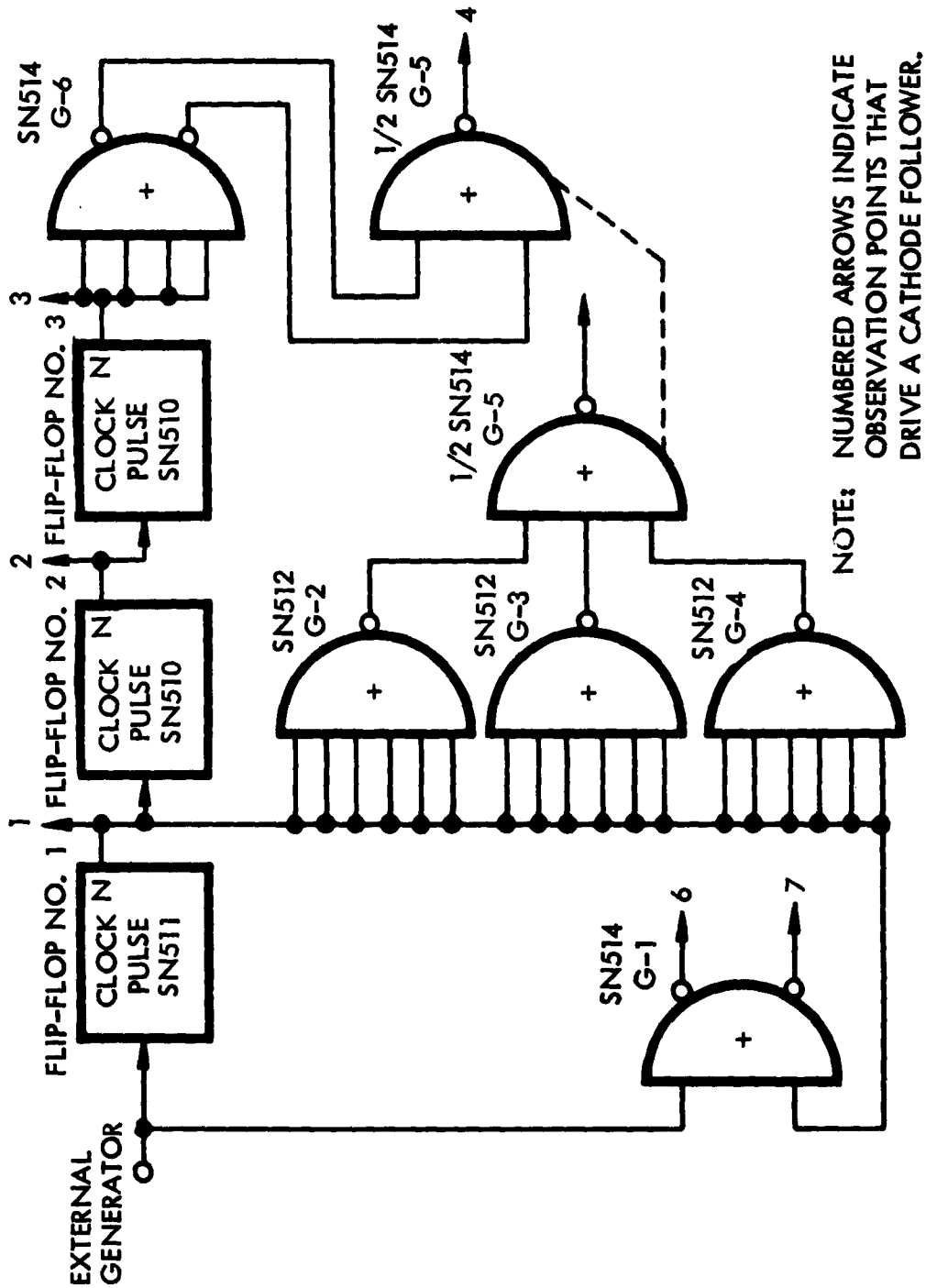

Figure 18. Circuit interconnection scheme.

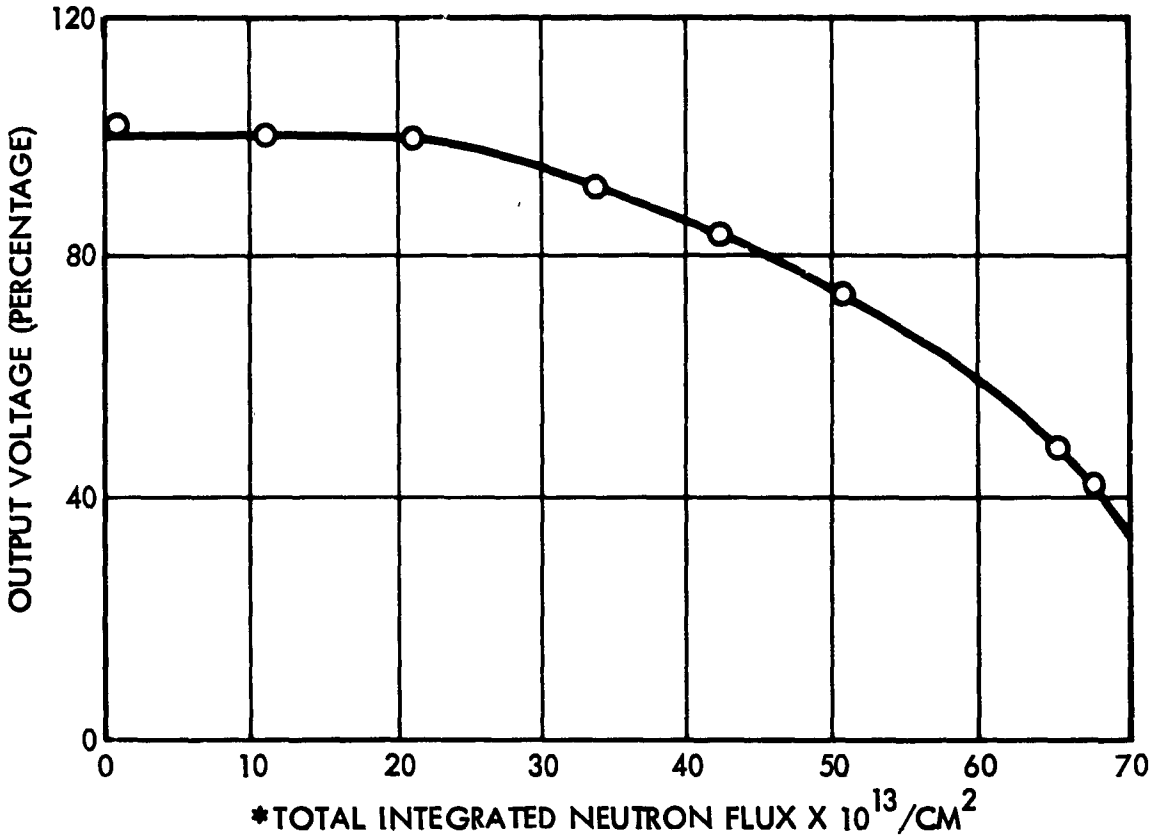

Figure 19. Output voltage change versus integrated neutron flux (SCIC three-input NAND gate).

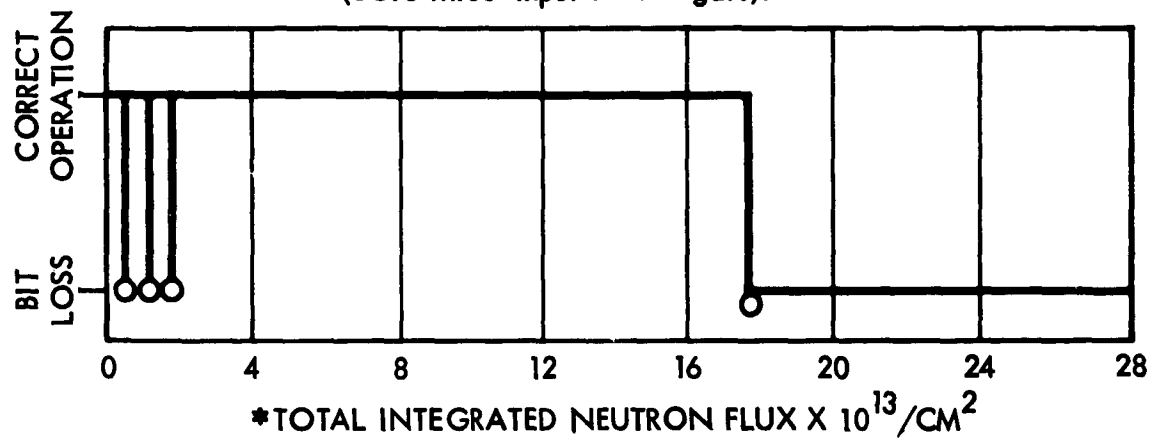

Figure 20. Bit loss versus integrated neutron flux (SCIC binary counter).

		MULTIPLY BY:
*1.	TOTAL NEUTRON FLUX	1.000
2.	THERMAL NEUTRON FLUX	0.499
3.	EPITHERMAL NEUTRON FLUX	0.499
4.	FAST NEUTRON FLUX (E_n > 2.9 MEV)	0.002
5.	GAMMA-RAY DOSE	$1.42 \times 10^{-5} R \frac{CM^2}{N}$

ABSTRACT 14: DOUGLAS AIRCRAFT COMPANY

"Neutron Damage to Integrated Circuits," private communication, October 1963

Author: Ahram Solimonian

An additional number of logic circuits were irradiated in the UCLA training reactor facility. The dosimetry was computed from a spectrum mapping done by UCLA using foil activation techniques. The circuits were irradiated while operating in a typical operating configuration. In some cases the output voltage and switching times were monitored using Nuvistor cathode followers to drive the 60 feet of coaxial cable required to reach the control room. For the systems performing logic functions, bit loss was monitored during irradiation. This loss occurred sporadically at lower levels, but eventually correct operation became impossible. The results are plotted against total neutron fluence. Table XI summarizes the circuits tested and the total integrated neutron flux required to give the degradation indicated. The thermal neutrons (energies less than 0.4 ev) represent 49.9 percent of the total while the fast flux (energies above 2.9 Mev) represents 0.2 percent of the total flux. The gamma dose has also been estimated. The output voltage refers to the logic swing rather than to a particular logic level.

Table XI. Summary of Neutron Damage

Microcircuit	Manufacturer	Total Integrated Neutron Flux ($\times 10^{13}$)	
		Output Voltage (50% Down)	Bit Loss (Complete)
Binary Counter	PSI	63	18
Delay Line Counter System	Signetics	---	138
SE100	Signetics	>160	---
SE120	Signetics	110	---
Adder Subsystem	Fairchild	---	82
µL "H"	Fairchild	290	---
µL "B"	Fairchild	>400	---
Counter System	Sylvania	---	420
M0057 and M0043 Gate	Sylvania	~500	---
MC306G	Motorola	120	---
Shift Register	GE	---	83
P324 and P325	GE	110	---

ABSTRACT 15: GENERAL ATOMIC

Technical Summary Report Jan. 16, 1964 to Feb. 14, 1964, General Atomic Document GACD-5134 (excerpts), March 29, 1965

Authors: J. W. Harrity and R. A. Poll

Eighteen Texas Instruments, fourteen Westinghouse, and one General Electric integrated microcircuits were tested in a linear-accelerator beam of 25- to 30-Mev electrons. Radiation doses varied from 0.1 to 500 rads (Si), and pulse widths varied from 0.1 to 1 microsecond. Dose was monitored by integrating the signal from a secondary-emission monitor.

Output voltages and currents were monitored as a function of dose. Threshold radiation levels are reported for some of the types of circuits tested. The circuits include flip-flops, gates, switches, drivers, and amplifiers.

The Texas Instruments SN355 driver switch had about 20 amperes of current flowing through the circuit during the pulse. This current was limited by a 0.5-ohm resistor in the emitter lead of one of the output transistors to prevent burnout of the output transistors.

The flip-flops will change state at radiation levels of about 10 rads (Si). Higher doses saturate the flip-flops. Recovery is to the state determined by asymmetries in the circuit.

"Latchup"* was observed in some of the general-purpose amplifiers. Those that did not "latch up" exhibited long turnon times (tens of microseconds).

Two level-detector integrated circuits were destroyed by radiation-induced excess currents that caused burnout of an aluminum conductor strip.

The report consists of unclassified excerpts from report GACD-5134.

---

*Latchup is defined as sustained ionization-induced current assumed to be caused by coupling of adjacent components through the isolation layer.

ABSTRACT 16: GENERAL ATOMIC

Development of Radiation-Resistant Computer Circuitry, General Atomic Document GA-5460, July 27, 1964

Author: R. A. Poll

A number of American Bosch-Arma circuits consisting of word selector 1, word selector 2, prime driver, micro A flip-flop, and micro B flip-flop were tested. A Sylvania SFF2A flip-flop and a Texas Instruments SN530 flip-flop were also included in the tests. The radiation source was a linear accelerator operating at 25 to 30 Mev with pulse lengths from 0.1 to 4.5 microseconds and providing total doses from 0.1 to 12,000 rads (Si). Tables XII and XIII summarize these results.

The word selector 1, word selector 2, prime driver, micro A flip-flop, and SFF2A flip-flop were also tested in a neutron environment at TRIGA. Resistive loads were used in the tests. Table XIV summarizes the results.

Table XII. Summary of Power Supply Currents in Various Circuits

Circuit	Dose Rate	Current (ma)	Saturation Dose
Word selector 1	3.4×10^8 rad (Si)/sec^{-1}	30	
	2.1×10^9 rad (Si)/sec^{-1}	90	
	12,600 rad (Si)/4.2 μsec	480	
Word selector 2	2.6×10^8 rad (Si)/sec^{-1}	1.7	2,000 rads (Si)
	1.1×10^9 rad (Si)/sec^{-1}	6	
Prime driver	50 rad (Si)/sec^{-1}	40	100 to 200 rads (Si)
	70 rad (Si)/sec^{-1}	250	

Table XIII. Summary of Circuit Switching Levels

Circuit	Dose to Change State	Remarks
A flip-flop	1490 rad (Si)/4.2 μsec	Device saturates beyond this total dose.
B flip-flop	10 rad (Si)/0.1 μsec	Circuit malfunctioned.
SN530 flip-flop	7×10^{6} rad (Si)/sec^{-1}	Circuit malfunctions after several pulses; does not change to opposite state up to 10^{9} rad (Si)/sec^{-1}.
SFF2A flip-flop	1.2×10^{9} rad (Si)/sec^{-1}	Does not change to opposite state up to 1.6×10^{9} rad (Si)/sec^{-1}.

Table XIV. Summary of Permanent Damage Data

Circuit	Initial Degradation Dose (Nvt)	Remarks
Word selector 1	3×10^{13}	Circuit output degrades severely beyond this dose.
Word selector 2	1×10^{14}	Circuit output drops to 0 current before 10^{15} nvt.
Prime driver	1×10^{14}	Circuit degrades rapidly beyond 1×10^{14} nvt.
Micro A flip-flop	1×10^{14}	Circuit was not irradiated beyond 3×10^{14} nvt; increase in trigger voltage at 3×10^{14} not indicated; h_{FE} of transistors was dropping.
SFF2A flip-flop		Operates normally to 10^{15} n/cm^{2}.

ABSTRACT 17: GENERAL ATOMIC

Technical Summary Report Feb. 7, 1964 to May 6, 1964, General Atomic Document GACD-5584 (excerpts), March 29, 1965

Authors: J. W. Harrity and R. A. Poll

Radiation-induced power supply currents during and after the radiation pulse were measured in a linear-accelerator beam operating at 25 to 30 Mev. The pulse width varied from 0.1 to 4.5 microseconds, and the dose varied from 0.1 to 30,000 rad (Si)/pulse. The circuits tested are listed in table XV. Illustrations in the report show excess transient currents versus radiation dose for a number of the circuits studied. Table XVI is a summary of many of the circuits and lists their applied voltages, where available; the radiation thresholds; power supply currents observed at 200 rads; and the direction of current flow in the microcircuit. An attempt was made to determine the cause of the current for those integrated circuits where the layouts were available. Several failure mechanisms were tried to explain the observed currents.

Table XV. Integrated Circuits Tested

Description	Manufacturer	Equivalent No.
Demodulator chopper	Texas Instruments	SN354
Driver switch	Texas Instruments	SN355
Flip-flop	Texas Instruments	SN537
Flip-flop	Westinghouse	W2601
Logic flip-flop	Motorola	---
One-shot multivibrator	Motorola	---
General-purpose amplifier, mode 1	Texas Instruments	SN349
General-purpose amplifier, mode 2	Texas Instruments	SN351
General-purpose amplifier, mode 1	Westinghouse	W914
General-purpose amplifier, mode 2	Westinghouse	W916
General-purpose amplifier, mode 4	Westinghouse	W917
Input network	Texas Instruments	SN343
Level detector	Texas Instruments	SN336
Low-level switch	Texas Instruments	SN340
Low-level switch	Westinghouse	---
Matrix switch	Texas Instruments	SN348
902 NAND gate	Westinghouse	W2602
903 NAND gate	Westinghouse	W2603
903 NAND gate	Texas Instruments	SN341
904 NAND gate	Texas Instruments	SN347
904 NAND gate	Westinghouse	W2604
Output drivers (old model) (circuit No. 1)	Texas Instruments	SN346
Output driver (new model) (circuit No. 2)	Texas Instruments	
Power switch	Westinghouse	W921
Read preamplifier	Texas Instruments	SN342
Write switch	Texas Instruments	SN345

Table XVI. Radiation Thresholds and Power Supply Currents

Circuit Type	Substrate Type	Voltages	Threshold (rads Si)	Power Supply Current at 200 Rads (ma)	Current Flow
Demodulator chopper	n	*	*	*	
Flip-flop (Texas Instruments)	p	+6, grd, -3	6.3, 7.3	+6v, 300 grd, 100 -3v, 200	+6, → -3, grd
One-shot flip-flop (Motorola)		-6, +6, grd	*	+6v, 16 grd, 11 -6v, 31	grd, +6 → -6
Logic flip-flop (Motorola)		grd, +6	*	+6v, 120 grd, 100	+6 → grd
Flip-flop (Westinghouse)	p	+6, grd, -3	0.9	+6v, 650 grd, 350 -3v, 350	+6 → -3, grd
GPA mode 1 (Westinghouse)	p	-12, +6, grd	*	-12v, 200 +6v, 230	+6 → -12
GPA mode 2	p	-12, +12, +6, grd	"latchup" at 13 rads Si	-12v, 3.6 +6v, 7.2 grd, 1.1	+6 → -12, grd
Input network (Texas Instruments)	n	-3, grd, +24, +6	1.5	+24v, 1,800 +6v, 60 grd, 1,800 -3v, 70	+24, +6 → grd, -3

* Not available

Table XVI. Radiation Thresholds and Power Supply Currents (Continued)

Circuit Type	Substrate Type	Voltages	Threshold (rads Si)	Power Supply Current at 200 Rads (ma)	Current Flow
Level detector (Texas Instruments)	p	−12, −6, −3, grd, +3, +12	50 (for flipping states)	+12v, 310 −3v, 44 −6v, 120 −12v, 120	+12 → −12, −6, −3
Low-level switch (Texas Instruments)	p	grd, +6 −3	*	+6v, 80 grd, 16 −3v, 85	grd, +6 → −3
Low-level switch (Westinghouse)	n	grd, +6, −3	*	+6v, 130 grd, 95 −3v, 120	+6 → grd, −3
Matrix switch	n	+12, +6, grd, −6	94	+12v, 150 +6v, 420 −6v, 510 grd, 20	+6, +12 → grd, −6
902 NAND gate (Texas Instruments)	p	+6, grd, −3	6.4	+6v, 30 grd, −3v, 7	+6 → −3, grd
903 NAND gate (Texas Instruments)	p	+6, −3, grd	120 (one input grd, others open)	+6v, 180 −3v, 75 grd, 140	+6 → grd, −3

* Not available

Table XVI. Radiation Thresholds and Power Supply Currents (Continued)

Circuit Type	Substrate Type	Voltages	Threshold (rads Si)	Power Supply Current at 200 Rads (ma)	Current Flow
903 NAND gate (Westinghouse)	p	+6, grd, -3	*	+6v, 400 -3v, 110 grd, 0	+6 → 400 ma
904 NAND gate (Texas Instruments)	p	grd, +6, -3	12	+6v, 450 grd, 20 -3v, 350	+6 → -3
904 NAND gate (Westinghouse)	p	+6, grd, -3	*	grd, 0 +6v. 390 -3v, 380	+6 → -3
Output driver (old model, Texas Instruments)	n	+12, +6, -12	4.4	+12v, 620 +6v, 70 -12v, 620	+6, +12 → -12
Output driver (new model, Texas Instruments)	p	+12, +6, -12	0.1 to 9	+12v, 600 +6, 590 -12v, 940	+6, +12 → -12
Read preamplifier (Texas Instruments)	n	+9, -9	*	+9v, 300 -9v, 260	+9 → -9
Write switch, inputs open (Texas Instruments)	n	+6, +3, -3, grd	*	+6v, 30 grd, 16 -3v, not measured +3v, not measured	

* Not available

Table XVI. Radiation Thresholds and Power Supply Currents (Continued)

Circuit Type	Substrate Type	Voltages	Threshold (rads Si)	Power Supply Current at 200 Rads (ma)	Current Flow
Write switch, inputs tied to +3v, Serial No. 0415-6-7 (Texas Instruments)	n	+6, +3, -3, grd	12	+6v, 50 +3v, 80 -3v, 130	+6, +3 → -3
Write switch, inputs tied to +3v, Serial No. 0174 (Texas Instruments)	n	+6, +3, -3, grd	12	+6v, 350 +3v, 200 -3v, 350	+6, +3 → grd, -3

* Not available

ABSTRACT 18: GENERAL ATOMIC

Technical Summary Report May 15, 1964 to July 28, 1964,
General Atomic Document GACD-5854, November 19, 1964

Authors: S. J. Black, J. W. Harrity, R. A. Poll, et al.

Transient power supply currents were investigated in a linear accelerator operating at 25 to 30 Mev. Pulse widths were varied from 0.1 to 4.5 microseconds to obtain doses ranging from 0.1 to 10,000 rad/pulse.

Schematic diagrams, test circuit diagrams, and plots of radiation-induced current transients as a function of dose are given.

A number of integrated circuit resistors were also investigated; namely, ACT LAB resistors having various resistances and a Signetics PF-861T resistor. In all the units studied, the response was a linear function of dose to approximately 1,000 rad. No differences between the photocurrents were observed under different bias conditions. The apparent leveling off of radiation-induced signals at higher dose rates is due to the longer pulse widths where the output signals are proportional to the dose rate instead of to total dose. The longer pulse is required to obtain a higher dose level.

Table XVII lists the integrated circuits studied and gives radiation-induced currents observed in the power supply leads.

Table XVII. Radiation-Induced Power Supply Currents

Circuit	Manufacturer and Type	Power Supply		Dose (Rads Si) (0.1-μsec pulse)
		Applied Voltage	Radiation-Induced Current (ma)	
Driver switch (920E)	Texas Instruments SN355	+24v	400	100
		+6v	55	---
		Grd	200	---
		-6v	300	---
GPA (933E)	Texas Instruments SN351	+12v	12	100
		+6v	2	---
		Grd	2	---
		-12v	6	---
Level detector (912)	Texas Instruments SN336	+12v	140	108
		Grd	120	108
		-6v	80	97
One-shot multivibrator	Motorola (no type)	+6v	240	110,000[a]
		Grd	70	99,000[a]
		-6v	220	96,000[a]
Dual four-input TTL gate	Motorola (no type)	+6v (input grd)	120	108
		Grd (input grd)	130	92[b]
NAND gates (904)	Texas Instruments SN347	+6v (input grd)	1,200	3,700[b]
	Westinghouse W2604	+6v (input grd)	600	3,150[b]
Read preamplifier (911)	Manufacturer not stated (T. I. SN342 and a Westinghouse circuit tested)	+9v	450	1,200[b]
		Grd	150	
		-9v	600	
Write switch (908)	Manufacturer not stated (T. I. SN345 and a Westinghouse circuit tested)	+6v (input open)	24	115
		Grd (input open)	18	125

[a] 4.5-μsec pulse length

[b] 0.5-μsec pulse length

ABSTRACT 19: GENERAL ATOMIC

Statistical Tests on Electronic Components, General Atomic Document GACD-6092, January 23, 1965

Authors: L. Berry, S. Black, R. Denson, et al.

Statistical data on various components tested are presented in the form of plots of the various currents and voltages measured. The dose is delivered in a 0.1-microsecond pulse from a linear accelerator. The energy used is not given, but it is presumed to be 25 to 30 Mev.

Three groups of 901 flip-flops were tested, one group manufactured by Texas Instruments and two groups by Westinghouse. Three groups of 902 NAND gates were tested, one group from Texas Instruments and two groups from Westinghouse. Three groups of 908 write switches and one group of 909 matrix switches, all made by Texas Instruments, were tested. One group of 919 demodulator choppers, one group of 921 power switches, and a group of polyintegrated circuits, all manufactured by ACT Laboratory, were also tested.

Power supply surge currents and circuit output voltages are presented as a function of total dose, rads (Si), for each device.

Thresholds for the various circuits occurred at 4.5 to 5.5 rads for the Texas Instruments 901 flip-flop, 3.2 to 8.7 rads for the Westinghouse 901 flip-flop, 0.2 to 0.5 rads for the 908 write switches, and 3.5 to 6 rads for the output of the 919 demodulator chopper. No threshold data are available for the remaining circuits.

ABSTRACT 20: HONEYWELL, INC.

"Microcircuits Survive Van Allen Belt," Aviation Week & Space Technology 79, August 19, 1963, p. 10

This report states that semiconductor microcircuits produced by three different manufacturers have demonstrated sufficient resistance to neutron irradiation to indicate that they could operate for at least 100 years within or below the inner Van Allen belt if this type of radiation were the limiting factor on their lives.

The investigations centered on the permanent effects of integrated neutron fluxes up to 10^{15} n/cm^2.

Five groups of circuits were tested: four series-connected Signetics SE100T gates, four Fairchild "G" gates in tandem, two Texas Instruments SN514 gates in series, and two discrete component NAND gates. Five 2N708 transistors monitored transistor beta degradation.

The circuits were tested in the University of Florida 10-kw water-cooled cobalt reactor, which is capable of producing flux rates of 2×10^{11} n/cm^2/sec. The circuits were exposed in increments to gradually increasing flux rates so that circuit responses could be monitored at different rates as well as at different integrated doses.

The circuits were exposed to an integrated dose of 10^{15} n/cm^2, which corresponds to the dose they would receive in a continuous orbit of about 500 years duration within the inner Van Allen belt (total dose per year would be 2.2×10^{14} n/cm^2; about 3.6×10^{11} n/cm^2 for 1 hour of exposure to a solar flare near the earth).

At 2.8×10^{14} n/cm^2, an integrated dose that would be experienced only after about 100 years continuous exposure in the Van Allen belts, the output from the Texas Instruments microcircuit chain disappeared. At the end of the tests, the Fairchild chain showed some deterioration in wave shape, which was reflected as increased asymmetry in the output wave shape. Neither of the Signetics chains

(possibly because they used higher-speed transistors) nor the circuits using discrete components showed any deterioration.

ABSTRACT 21: HONEYWELL, INC.

Nuclear Radiation Study of Digital Logic Circuits, Engineering Test Report No. 8835, August 3, 1964

Author: G. E. Prow

Fourteen logic circuits were irradiated in the University of Florida training reactor. The devices tested were: two Honeywell D910617 DTL flip-flops, two Honeywell D911272 DTL flip-flops, one Signetics SE124K DTL flip-flop, one Signetics SE150K DTL line driver, one Texas Instruments SN533 DCTL dual three-input gate, one Motorola SC340 TTL eight-input gate, one Fairchild μC 103 TTL dual four-input gate, two Sylvania SNG4 TTL dual three-input gates, and three Fairchild μL900(B) DCTL buffers. Measurements were of logic level voltages and switching times. No significant changes were observed to a fluence of 9.4×10^{14} n/cm^2 (2.3×10^{13} n/cm^2 of $E_n > 3.0$ Mev) and 2.0×10^6 R gamma rays.

ABSTRACT 22: HONEYWELL, INC.

Nuclear Radiation Study of Digital Integrated Circuits, Test No. 2, Engineering Test Report No. 8838, Memoranda dated December 22, 1964, and February 28, 1965

Author: G. E. Prow

A number of circuits and components were irradiated in the University of Florida training reactor. The circuits included Texas Instruments SN1119 and SN1118, Fairchild μC103 and μL900, Signetics SE124K, and Honeywell ES1001. Two transistors from Texas Instruments, SN1118 and μL900, monitored h_{fe}. The significant quantities measured were minimum 1-level output voltage and maximum 0-level output voltages, 0- and 1-level threshold output voltages, rise time, fall time, and propagation time. Rise and fall times were taken between 1- and 2-volt levels. Propagation times were taken at the 50-percent level. Propagation times degraded in the Texas Instruments SN1119 and Fairchild μC103 circuits. (The propagation time was not monitored in the remaining circuits.)

Degradation of noise immunity versus neutron dose for the Texas Instruments SN1119 and Fairchild μC103 circuits is presented in the report, along with data showing the degradation of h_{fe} as a function of dose for the transistors used.

The Honeywell ES1001 failed before 3.5×10^{12} nvt and 2.5×10^{3}R, presumably due to SCR failure. No failures were observed in DTL and TTL circuits before 6.8×10^{13} nvt and 4.9×10^{6}R, as monitored by coincidence logic at a bit rate of 20 kilocycles and a 50-percent duty cycle. All of these neutron doses were for energies greater than 3 Mev (sulfur foil dosimetry was used).

ABSTRACT 23: HUGHES AIRCRAFT COMPANY

Radiation Effects on Guided Missile Electronic Equipment, FR 63-17-173, July 15, 1963

Authors: J. E. Bell and R. W. Marshall

Several integrated monolithic and thin-film circuits were tested for their response to transient ionizing radiation. Bremsstrahlung generated by a 10-Mev electron beam from the Hughes research linear accelerator was used as the radiation source. The integrated circuits tested included the Texas Instruments SN510 flip-flop, the Fairchild micrologic flip-flop, the Fairchild micrologic gate, the Signetics SE102K logic gate, the Philco μ7006 gate, an experimental Melpar thin-film bistable network, and an experimental Melpar thin-film 4-kilocycle oscillator circuit.

The Texas Instruments SN510 flip-flop and SN514 dual logic gate were also subjected to neutron dose radiation at the Sandia pulsed reactor facility (SPRF). Two SN510 flip-flops failed after a combined integrated dose of 3.5×10^{12} n/cm^2 (sulfur) and 1×10^4R gamma-ray exposure. Two SN514 circuits were irradiated to a combined dose of 8.5×10^{12} n/cm^2 (sulfur) and 2.5×10^4R of gamma rays. The turn-on voltage threshold increased from 0.47 to 0.72 volts during irradiation, while the output voltage decreased from 4.7 to 3.2 volts. Loading capabilities were not determined for either of the circuits.

Transient radiation switching thresholds for the SN510 flip-flop are summarized below:

Transistor T1	Transistor T2	Minimum Gamma Exposure Rate Required for Change in State (R/sec)
OFF	ON	0.4×10^6
ON	OFF	6.0×10^6

A Fairchild micrologic flip-flop was tested while operating at a 1.2-megacycle rate. At exposure rates greater than 2×10^7 R/sec, the flip-flop did not operate properly. The Fairchild micrologic gate and the Signetics SE102K gate were tested simultaneously at various transient radiation rates with the gates connected in the normally off state. Output voltage was monitored during the tests. The Fairchild gate was more sensitive than the Signetics gate. The threshold for the Signetics gate was nearly equal to 10^8 R/sec. No loads were used in the tests. The Philco μ7006 gate response was about 20 percent lower than the Signetics SE102K at 7.5×10^7 R/sec when they were biased in the "off" condition.

Two experimental circuits were constructed, one from two bulk semiconductor resistors (Fairchild μER-2) and a bulk semiconductor transistor (Fairchild μET-1) with the isolation diodes connected to ground, and the other from two thin-film resistors and a bulk semiconductor transistor (Fairchild μET-1) with the isolation diode floating. The transistors were in separate TO-5 cans, as were the semiconductor resistors. The thin-film resistors were mounted on the top of the TO-5 cans containing the semiconductor resistors. The transient response from the bulk semiconductor circuit was 10 times that of the hybrid circuit at 1×10^8 R/sec. The transient response of the hybrid circuit was increased 30 times by grounding the isolation diode.

The thin-film bistable circuit would not change state for exposure rates up to 1×10^8 R/sec gamma rays with pulse lengths varying from 1 to 6 microseconds and for electrons (6 Mev at 350 ma) up to about 10^{10} to 10^{11} R/sec. Other configurations of the circuit (loading, grounding outputs, etc.) were unstable.

Data were obtained for the 4-kilocycle oscillator while the oscillator was in operation. The oscillator period was long compared to the linear-accelerator pulse. Fast- and slow-ordered amplitude responses were found to be rate dependent.

Thin-film and bulk semiconductor components were tested in the gamma-ray pulse. Both shunt current and injected currents were an order of magnitude larger for bulk semiconductor resistors. Thin-film resistors had no measurable effects due to transient radiation up to 1×10^8 R/sec. Thin-film capacitors showed effects

similar to the thin-film resistors. Capacitors were rated as to dielectric leakage during the radiation pulse. Zinc-sulfide dielectrics exhibited the greatest amount of current leakage, silicon-dioxide and silicon-nitride dielectrics were less leaky, and ceramic materials showed no measurable leakage. Metal-oxide semiconductor (MOS) capacitors were tested, but no definite conclusions could be elicited from the results.

Integrated circuit transistors were tested with and without the substrate grounded. The results are summarized in table XVIII.

Table XVIII. Results of Integrated Circuits Tested

Transistor Type	No. 1 μET-1 (ma)	No. 1 μET-2 (ma)	No. 2 PF801T (ma)	No. 6 PF801T (ma)	No. 2 PF800T (ma)	No. 6 PF800T (ma)
Substrate not grounded	0.03	0.04	0.025	0.03	0.32	0.09
Substrate grounded	0.32	0.40	0.14	0.12	0.42	0.11
Ratio = Grounded / Ungrounded	10.7 / 1	10 / 1	5.6 / 1	4 / 1	1.3 / 1	1.2 / 1

Some preliminary tests were made on field-effect transistors (FET), the results of which indicated that some of the p-n junction planar types have transient radiation responses at dose rates as low as 1×10^6 R/sec. Thin-film, insulated-gate, FET's indicate very little response at dose rates up to 1×10^8 R/sec.

ABSTRACT 24: JOHNS HOPKINS UNIVERSITY APPLIED PHYSICS LABORATORY

"Evaluation of Texas Instruments Series 51 Integrated Circuits In a Co^{60} Radiation Environment," private communication, April 1965

Authors: R. Coopeman and G. Wagner

The Applied Physics Laboratory has been evaluating Texas Instruments Series 51 integrated circuits for use in several satellites by subjecting them to Co^{60} gamma radiation. The circuits were purchased from distribution stocks and were irradiated without prior burn-in; they included four SN514A, two SN513A, and two SN511A.

The integrated circuits were soldered onto 1/16-inch fiberglass printed circuit cards (two circuits per card) and irradiated at a dose rate of 7×10^4 rads/hr under a static bias of +4 volts dc. At logarithmic time intervals, the circuits were removed from the Co^{60} radiation and the following parameters were measured:

SN514A and SN513A Gates	SN511A Flip-Flops
β_{AC} (at 4 kc and 0.8 ma)	Clock-pulse sensitivity
β_{DC} (at 0.8 ma)	Preset-pulse sensitivity
I_{CBO} (at 4 vdc)	t_r
B_{VCES}	t_f
t_r	Output logic voltages
t_f	
V_{off} for (V_{on}) max.	
V_{on} for (V_{off}) min.	

Up to an integrated dose of 2.35×10^7 rads, only one failure occurred. This was an SN513A gate, which had leakage currents that were sufficient at 1.32×10^7 rads to drop the collector voltage below the V_{off} specification and at 2.35×10^7 rads to saturate the gate. The leakage currents of this particular gate at the end of the test were an order of magnitude greater than that found in any of the others. All other circuits performed properly and easily met manufacturer's

specifications. Throughout the tests the only significant changes noted were a rapid fall in ß and a large increase in I_{CBO}; operationally, from a circuit building-block viewpoint, there was no significant change. Preliminary data are available that give the results of each measurement as a function of dose from 10^4 to 2.35×10^7 rads.

ABSTRACT 25: LING-TEMCO-VOUGHT

Radiation Effects on Thin-Film Microelectronics, ME-RD3R-2, March 31, 1964

Author: John Vesecky

Various thin-film circuit components were exposed to approximately 10^{16} fast neutrons/cm^2 and 3×10^8 R gamma rays at a temperature of 90°C in the General Dynamics reactor at Fort Worth, Texas. Components irradiated included vacuum-deposited thin-film nichrome resistors; nichrome-SIO dielectric capacitors on soda-lime glass using sputtered and etched tantalum for one electrode, anodized tantalum for the dielectric, and gold for the counter electrode.

Electrical measurements were made before and after irradiation and included the resistance, Q at 1,000 cycles, and dielectric insulation resistance where appropriate. Control resistors were also included in the resistor tests.

The results for resistors show that as the resistance increases, the effect of irradiation is greater. In the SIO capacitors, the capacitance changed a small amount (mean change 1.3 percent), the Q increased an average of 19 percent, and the insulation resistance increased an average of 65 percent. The results for the anodized tantalum capacitors are erratic, because some of the capacitors were defective to begin with. Regarding the anodized capacitors, it can be concluded that with radiation the capacitance increases slightly, Q increases, and the insulation resistance drops slightly.

ABSTRACT 26: LITTON SYSTEMS, INC.

Radiation Effects Upon Digital Integrated Circuits and Support, June 1964

Authors: Alvin B. Kaufman and Harry R. Newhoff

The dual four-input NAND/NOR gates (PHOENIX LINC) of various manufacturers and a number of milliwatt logic circuits were exposed to 1.2×10^{14} n/cm^2 ($E_n > 10$ kev) at the General Atomic Mark I reactor and to 10^8 R/sec at the Hughes Aircraft Company linear accelerator.

The logic levels and switching times of the circuits for various fanouts were measured before and after the neutron test.

The neutron dosimetry was performed using foil activation techniques. The circuits were shielded from thermal neutrons by a cadmium shield. LINC circuit failures are summarized in table XIX; table XX lists the milliwatt logic circuits tested. In most of these circuits significant neutron damage was observed at -55°C, but no effect was observed at +25°C and +125°C.

The transient tests were conducted with four similar circuits driving one another serially (ie., fanout 1). The first three outputs were monitored. The linear-accelerator dosimetry was done using glass rods calibrated at a Co^{60} source. Tolerance of the LINC circuits to this ionizing radiation is also summarized in table XIX.

Table XIX. Summary of the Usability of LINC Circuits

Manufacturer	Permanent Damage		Transient Tolerance	Satisfactory for Both Environments
	Fanout = 15	Fanout = 5		
Fairchild	X	X	X	Unqualified Yes
Motorola	X	X	F	No
GME	F	X	X	Qualified Yes
Sylvania	F	X	X	Qualified Yes
Philco	F	X	F	No
Signetics	NT	NT	F	No
Texas Instruments	NT	NT	F	No

Legend: X: Passed
F: Failed where failure is based on the criteria that (a) the output level(s) was not within tolerance under the specified operational condition (i.e., the output was below 0.5 volt) or (b) the transient noise was of such a level that it exceeded the value necessary to trigger another associated circuit of the same basic characteristics (i.e., these units had greater than 0.5-volt transient output).
NT: Not tested

Table XX. Milliwatt Logic Circuits Tested

Manufacturer	Circuit
Fairchild	Dual two-input type 910 milliwatt logic gate
Philco	Single four-input type 911 milliwatt logic gate
Fairchild	Type 913 milliwatt logic shift register
GME	Type 913 milliwatt logic shift register

ABSTRACT 28: LOCKHEED MISSILES AND SPACE COMPANY

"Radiation Tests of Fairchild Products," private communication, August 4, 1964

Author: J. W. Cecil

The Fairchild DT μL931 flip-flop was irradiated with 20-nanosecond pulses of 150-kev X rays at the Physics International flash X-ray facility. The state of the flip-flop was not observed to have changed after any shot. Exposure rates varied from 2.5×10^8 to 2×10^9 R/sec.

ABSTRACT 29: MOTOROLA

"Radiation Tolerance of Integrated Circuits," Unpublished memorandum, March 18, 1964

Author: J. Flood

Seven integrated circuit test patterns containing a transistor similar to a 2N918 transistor and resistors from 1.7 to 5.2 kilohms were irradiated in a gamma source (Co^{60}) to a dose of 3.48×10^6R. Parameters measured were h_{FE} at V_{CE} = 5 volts and I_c = 1 milliampere, I_{CBO} at V_{CB} = 20 volts, BV_{CBO} at I_c = 100 microamperes, resistance R at I_R = 1 milliampere, collector substrate leakage I_{cs} at V_{cs} = 10 volts.

The transistor h_{FE} and I_{CBO} changed significantly, as did I_{cs}. The mean increase in I_{CBO} was 4.5 nanoamperes, and the mean decrease in normalized h_{FE} was 0.14. I_{CBO} began degrading with irradiation, whereas h_{FE} remained constant to approximately 2×10^5R before degradation began. Resistors all increased in resistance slightly. Collector-base breakdown voltages showed only random fluctuations. I_{cs} increased approximately an order of magnitude during the irradiation.

ABSTRACT 30: NASA-LANGLEY RESEARCH CENTER

"Experimental Investigation of Simulated Space Particulate Radiation Effects on Microelectronics," paper presented at the Conference on Nuclear Radiation Effects, jointly sponsored by IEEE, the Professional and Technical Group on Nuclear Science, and the University of Washington, Seattle, Washington, July 20-23, 1964 (Battelle REIC Abstract 25533)

Authors: E. Rind and F. R. Bryant

Space radiation environments are briefly summarized. Proton irradiation data at 22, 40, 128, and 440 Mev are presented for typical microelectronic components such as low-, medium-, and high-frequency transistors and compared with similarly irradiated discrete- and integrated-circuit types of microcomponents. Damage tends to vary inversely with energy. Integrated flux levels of approximately 10^{11} protons/cm^2 are needed before the radiation effects become noticeable. Integrated circuits appear to be slightly more resistant to radiation, but this finding may not be significant on a statistical basis.

ABSTRACT 31: NORTHROP-VENTURA

"Integrated Circuit Experimental Investigation," Interoffice communication 2240/64-14

Author: J. Raymond and E. Steele

A number of Westinghouse, Fairchild, and Signetics integrated circuits and components were exposed to radiation environments of up to 5×10^6 R/sec at the Northrop Ventura 600-kev flash X-ray machine and from 10^{12} to 10^{15} n/cm^2 fast neutron fluences ($E_n > 10$ kev) at the Northrop TRIGA reactor. The dosimetry in each case was related to previous mappings using a photodiode dosimeter at the flash X-ray facility and foil activation techniques at TRIGA.

In the flash X-ray experiments the transient circuit disturbance was measured by monitoring the voltage transient at a critical circuit node. High-impedance instrumentation was used to avoid parasitic circuit loading. The circuits were investigated statically (i.e., biased at a fixed operating point with no dynamic applied signal). The results are shown in table XXI.

The response of the SE115 is 30-percent greater when internally loaded with a resistor than when externally loaded with a resistor; this illustrates the importance

Table XXI. Flash X-ray Circuit Response

Circuit	Output Logic	Turnon Output Volts	Change in Output Current for On and Off State
W2101 DTL dual NAND/ NOR gate (Westinghouse)	Off	50-75 mv	30 μa (0.1 μa normal current)
SE115 DTL dual NAND/ NOR gate (Signetics)	On	5 mv	—— (2 ma normal current)
"G" RTL gate (Fairchild)	Off	——	400 μa
	On	Small	——
W2102 flip-flop (Westinghouse)			Similar to gate response (no logic change)
SE121T flip-flop (Signetics)	Off		
μL902 flip-flop (Fairchild)	On		

of the substrate junction to the radiation response.

Circuits investigated for permanent damage in the neutron environment were a Fairchild "G" RTL gate, a Signetics 102K DTL NAND/NOR gate, and a Signetics 124K flip-flop.

The unloaded operating characteristics were measured at room temperature after each exposure. The range of total integrated neutron dose (greater than 10 kev) was from 10^{12} to 10^{15} n/cm^2. In all cases circuit performance was substantially degraded at 10^{15} n/cm^2. The degree of degradation was dependent on the sensitivity of the circuit operation to transistor gain degradation.

Transistor and resistor elements obtained from Signetics, simulating those employed in the integrated circuit, were evaluated at the flash X-ray facility. The substrate-collector and collector-base junction photocurrents were measured independently and then simultaneously for the transistor. At a constant-junction reverse bias of 3 volts, the measured response to a pulse having a peak intensity of approximately 2×10^6 R/sec was as follows:

Peak observed primary photocurrent: 25 microamperes

Peak observed substrate photocurrent: 50 microamperes

Peak observed combined photocurrent: 50 microamperes

These results imply that the substrate junction is closely coupled to the collector-base junction.

The change in conductivity and peak photocurrent measured in a 12- and a 20-kilohm integrated circuit resistor element (Signetics Pre-Feb type PF 861T) at a peak dose rate of 2×10^6 R/sec and pulse width of 0.2 microsecond was:

	20K Resistor	15K Resistor
Resistor change	64 ohms	40 ohms
Substrate photocurrent	65 microamperes	54 microamperes

ABSTRACT 32: TEXAS INSTRUMENTS, INC.

Radiation Effects on Solid Circuit Networks Series 51, SP23-A63, September 6, 1963 (Battelle REIC Abstract 24554)

A preliminary investigation of the damaging effects of radiation on Texas Instruments Solid Circuit Networks Series 51 has been performed. The objectives of the study are (1) to relate and compare the performance of SN511's to that of comparable transistors and transistor circuits and (2) to interpret the data in terms of a worst-case approximation for the useful lifetimes in a space radiation environment. The experiments selected for the study were the following: (1) exposure to 200-kev bremsstrahlung X rays, (2) irradiation by 6-Mev electrons, and (3) bombardment by 22-Mev protons. Only a few samples were used in each experiment, but the data are sufficiently consistent to justify the following interpretations and conclusions. SN511's are no more sensitive to a radiation environment than are similar conventional circuits containing medium-speed transistors. The mean particle fluxes to cause failure of the test samples were approximately 10^{13} protons/cm^2 and 5.5×10^{14} electrons/cm^2.

ABSTRACT 33: U. S. ARMY ELECTRONICS LABORATORIES

Private communication, April 1965

Authors: R. Farlee and E. T. Hunter

A flip-flop and an MECL three-input gate were tested at the Sandia pulsed reactor facility (SPRF) and the White Sands gamma-ray linear accelerator. Transient measurements were made during the radiation pulse. Output waveform was monitored. The gate was driven by a square pulse 12.5 microseconds wide, and the flip-flop was triggered by a clock pulse at 40 kilocycles per second. The loads were 75-ohm cable-terminating resistors. Gamma radiation caused the flip-flop to go on from both outputs. During radiation the gate was held at -1.5 volts (the low state). The radiation levels attained were 6.5×10^6 R/sec on the linear accelerator and 3 to 6×10^7 R/sec plus 10^{13} nvt at SPRF. Dosimetry was performed using sulfur foils and glass rods.

ABSTRACT 34: U. S. NAVAL RADIOLOGICAL DEFENSE LABORATORY

Private communication, March 1965

Authors: C. Ramstedt and H. Zagorites

A number of Melpar thin-film circuits using thin-film transistors were irradiated with Co^{60} gamma rays. The transistors were CdS n-channel devices with SiO insulators, aluminum gates, and nichrome electrodes. The circuits were potted in a silicon compound or in vacuum. Drain current and cutoff voltage were monitored. Radiation levels were 1.6×10^5 and 10^6R. No effects were observed at these exposure levels.

UNCLASSIFIED
Security Classification

DOCUMENT CONTROL DATA - R&D

(Security classification of title, body of abstract and indexing annotation must be entered when the overall report is classified)

1. ORIGINATING ACTIVITY *(Corporate author)*
THE BOEING COMPANY
Aero-Space Division
Seattle, Washington

2a. REPORT SECURITY CLASSIFICATION
UNCLASSIFIED/S-RD Supplement

2b. GROUP
S-RD Supplement: GP 1

3. REPORT TITLE
A SURVEY OF TRANSIENT RADIATION-EFFECT STUDIES ON MICROELECTRONICS

4. DESCRIPTIVE NOTES *(Type of report and inclusive dates)*
Survey Report (January through April 1965)

5. AUTHOR(S) *(Last name, first name, initial)*
Bowman, William C.
Caldwell, Robert S.
Svetich, G. W.

6. REPORT DATE	7a. TOTAL NO. OF PAGES	7b. NO. OF REFS
May 1965	128 + suppl 14	-

8a. CONTRACT OR GRANT NO.	9a. ORIGINATOR'S REPORT NUMBER(S)
AF30(602)-3585	
b. PROJECT NO. 5710	
c.	9b. OTHER REPORT NO(S) *(Any other numbers that may be assigned this report)*
d.	RADC-TR-65-147

10. AVAILABILITY/LIMITATION NOTICES All distribution of this report is controlled. Qualified DDC users will request through RADC (EMEAS), GAFB, NY. Foreign announcement and dissemination of this report by DDC is not authorized.

11. SUPPLEMENTARY NOTES	12. SPONSORING MILITARY ACTIVITY
NWER Subtask 16.027	Headquarters Defense Atomic Support Agency Washington, DC

13. ABSTRACT In order to obtain complete up-to-date knowledge of the work accomplished and presently being done on the effects of transient nuclear radiation on microelectronics, a survey of the laboratories investigating this subject was conducted. Telephone contacts were made with specific individuals in 53 different laboratories. Data were obtained by means of questionnaires, reports, and personal visits. Abstracts of each document or other data source are included in the report. The abstracts describe the devices tested and the test environment, the type of dosimetry used, the general results obtained, and provide other relevant information. Summaries of failure levels are given in the abstracts whenever the information was readily available. A tabulated summary of the devices tested and the test conditions is presented. Failure levels observed by different investigators are compared for a few duplicated devices. Nine classified abstracts are contained in a supplement to the main report.

DD FORM 1 JAN 64 1473

UNCLASSIFIED
Security Classification

14. KEY WORDS	LINK A		LINK B		LINK C	
	ROLE	WT	ROLE	WT	ROLE	WT
Survey Radiation Effects Microcircuits						

INSTRUCTIONS

1. ORIGINATING ACTIVITY: Enter the name and address of the contractor, subcontractor, grantee, Department of Defense activity or other organization *(corporate author)* issuing the report.

2a. REPORT SECURITY CLASSIFICATION: Enter the overall security classification of the report. Indicate whether "Restricted Data" is included. Marking is to be in accordance with appropriate security regulations.

2b. GROUP: Automatic downgrading is specified in DoD Directive 5200.10 and Armed Forces Industrial Manual. Enter the group number. Also, when applicable, show that optional markings have been used for Group 3 and Group 4 as authorized.

3. REPORT TITLE: Enter the complete report title in all capital letters. Titles in all cases should be unclassified. If a meaningful title cannot be selected without classification, show title classification in all capitals in parenthesis immediately following the title.

4. DESCRIPTIVE NOTES: If appropriate, enter the type of report, e.g., interim, progress, summary, annual, or final. Give the inclusive dates when a specific reporting period is covered.

5. AUTHOR(S): Enter the name(s) of author(s) as shown on or in the report. Enter last name, first name, middle initial. If military, show rank and branch of service. The name of the principal author is an absolute minimum requirement.

6. REPORT DATE: Enter the date of the report as day, month, year; or month, year. If more than one date appears on the report, use date of publication.

7a. TOTAL NUMBER OF PAGES: The total page count should follow normal pagination procedures, i.e., enter the number of pages containing information.

7b. NUMBER OF REFERENCES: Enter the total number of references cited in the report.

8a. CONTRACT OR GRANT NUMBER: If appropriate, enter the applicable number of the contract or grant under which the report was written.

8b, 8c, & 8d. PROJECT NUMBER: Enter the appropriate military department identification, such as project number, subproject number, system numbers, task number, etc.

9a. ORIGINATOR'S REPORT NUMBER(S): Enter the official report number by which the document will be identified and controlled by the originating activity. This number must be unique to this report.

9b. OTHER REPORT NUMBER(S): If the report has been assigned any other report numbers *(either by the originator or by the sponsor)*, also enter this number(s).

10. AVAILABILITY/LIMITATION NOTICES: Enter any limitations on further dissemination of the report, other than those imposed by security classification, using standard statements such as:

(1) "Qualified requesters may obtain copies of this report from DDC."

(2) "Foreign announcement and dissemination of this report by DDC is not authorized."

(3) "U. S. Government agencies may obtain copies of this report directly from DDC. Other qualified DDC users shall request through _____."

(4) "U. S. military agencies may obtain copies of this report directly from DDC. Other qualified users shall request through _____."

(5) "All distribution of this report is controlled. Qualified DDC users shall request through _____."

If the report has been furnished to the Office of Technical Services, Department of Commerce, for sale to the public, indicate this fact and enter the price, if known.

11. SUPPLEMENTARY NOTES: Use for additional explanatory notes.

12. SPONSORING MILITARY ACTIVITY: Enter the name of the departmental project office or laboratory sponsoring *(paying for)* the research and development. Include address.

13. ABSTRACT: Enter an abstract giving a brief and factual summary of the document indicative of the report, even though it may also appear elsewhere in the body of the technical report. If additional space is required, a continuation sheet shall be attached.

It is highly desirable that the abstract of classified reports be unclassified. Each paragraph of the abstract shall end with an indication of the military security classification of the information in the paragraph, represented as *(TS), (S), (C), or (U)*.

There is no limitation on the length of the abstract. However, the suggested length is from 150 to 225 words.

14. KEY WORDS: Key words are technically meaningful terms or short phrases that characterize a report and may be used as index entries for cataloging the report. Key words must be selected so that no security classification is required. Identifiers, such as equipment model designation, trade name, military project code name, geographic location, may be used as key words but will be followed by an indication of technical context. The assignment of links, rules, and weights is optional.

IMPLICATION FOR FUTURE WORK

The work here reported has shown that the classical hypothesis of tonotopic organisation in the primary auditory cortex of the cat is untenable. This, together with behavioural work which has been carried out on cats after cortical ablations, suggests that frequency discrimination may not be one of the major functions of the cortex. Two new properties of auditory cortical units have, however, been observed: (a) the existence of 'orientation units' which respond to one particular sequence of frequencies, but not to some other sequence and (b) the tendency of units to change their response patterns with time, these changes not being all of the same type.

In future work an attempt will be made to find, by applying appropriate stimuli, what kinds of temporal pattern, besides those already discovered, can be uniquely recognized by individual units. The possibility of classifying such units with respect to their position in the cortex will also be examined.

Concomitantly we propose to study, where possible, the response patterns of such units over long periods to see how these response patterns vary with time, and whether it is possible to 'train' units to give certain types of response, or change their response in predictable ways by suitable choice of stimuli.

Personnel Utilised

Title	Number of Hours devoted to this Contract
Graduate Investigator	Full-time
Technical Assistant	Full-time
Director	1/8 full-time
Secretarial Assistant	1/5 full-time

Materials

Expendable supplies and materials	£300. 0. 0.
Overhead costs	£450. 0. 0.
Property acquired	Nil.